University of Rijeka

Department of Physics

Expected number of neutrino interactions in the far detectors of the ESSnuSB project

Leon Halić

Master's Thesis

Rijeka, 2021

University of Rijeka

Department of Physics

Graduate Study Programme in Physics, Astrophysics and Elementary Particle Physics

Expected number of neutrino interactions in the far detectors of the ESSnuSB project

Leon Halić

Master's Thesis

Mentor: dr. sc. Budimir Kliček

Co-mentor: doc. dr. sc. Saša Mićanović

Rijeka, 2021

Contents

Abstract

ESSνSB is a project in a design phase with an aim to measure CP violation in lepton sector by observing neutrino oscillations. It consists of near detectors at 250 m from the neutrino production target and far detectors at 540 km (or 360 km) from neutrino production target. To make all the necessary simulations and analysis of the possible performance of ESSνSB experiment, one needs to know the expected number of neutrino interactions in all detectors of the experiment. This thesis provides expected number of neutrino interactions for near and far water Cherenkov detectors and near scintillator based detector. While calculating the neutrino oscillation probabilties, matter effects were taken into the account and compared to the vacuum oscillations. Comparison between expected number of interactions for different δ_{CP} values has been made, clearly demonstrating sensitivity to δ_{CP}. It is shown that the results do not depend much on the matter effects.

Key words: ESSνSB, neutrino oscillations, CP violation, neutrino interactions

1 Introduction

Standard Model of particle physics (SM) is a theoretical formulation which describes three of the four fundamental interactions (electromagnetism, weak and strong nuclear interactions) as well as all of the known elementary particles. These particles are further classified into fermions and bosons, where fermions are defined as particles with half-integer spin while bosons are defined as particles with integer spin. Each of the fundamental interactions is mediated by a vector boson. For electromagnetism (EM) it is a photon, for weak interaction these are $W^{\pm}$ and Z^0 bosons and for strong interaction these are the gluons.

$$\begin{pmatrix} u \\ d \end{pmatrix}, \quad \begin{pmatrix} c \\ s \end{pmatrix}, \quad \begin{pmatrix} t \\ b \end{pmatrix}$$

Figure 1.1: Three generations of quarks: up (u), down (d), charm (c), strange (s), top (t) and bottom (b).

Fermions are then further classified into quarks (see Fig. 1.1) and leptons (see Fig. 1.2), where the distinction lies in the fact that quarks interact via strong force and leptons do not. Both are grouped into three generations where for leptons we refer to those generations by the flavour of the charged leptons (electron, muon and tau) while the corresponding neutral leptons (neutrinos) are named after their charged counterpart (electron neutrino, muon neutrino and tau netrino). Neutrinos, having no electrical charge, interact with other particles only via the weak interaction by exchanging the $W^{\pm}$ and Z^0 bosons in which case the processes are called charged-current interactions (CC) and neutral-current interactions (NC), respectively.

$$\begin{pmatrix} e \\ \nu_e \end{pmatrix}, \quad \begin{pmatrix} \mu \\ \nu_\mu \end{pmatrix}, \quad \begin{pmatrix} \tau \\ \nu_\tau \end{pmatrix}$$

Figure 1.2: Three generations of leptons: electron (e), electron neutrino (ν_e), muon (μ), muon neutrino (ν_μ), tau (τ) and tau neutrino (ν_τ).

Neutrino has a reputation of causing problems for the established Standard Model. As its weak interactions are a problem in probing its properties, some mysteries still remain unsolved. The most famous of mysteries is the mass of a neutrino. There is a lot of evidence (such as neutrino oscillations) that neutrinos do indeed have mass, but its origin remains unknown. Second famous mystery is the CP symmetry violation, which is a focus of this thesis. In analogy with CP symmetry breaking in weak interactions of quarks, it is expected that neutrino interactions also break CP symmetry, but this, at the time of the writing, is still not observed. [1]

2 Theoretical background

2.1 Neutrino mixing

When the Standard Model was being formulated, knowledge about neutrinos was very limited. As a result of the available information, it was assumed neutrinos are masseless. In such a theory, the flavour neutrino fields (electron, muon and tau) are also mass eigenstates as any combination of massless fields is a also a massless field [2].

Since then, experiments have shown evidence of the opposite, that neutrinos indeed do have mass as predicted by the observation of neutrino oscillations (see section 2.2). First mathematical formulation of such phenomenon came form Maki, Nakagawa and Sakata [3] where they postulated that the flavour neutrino fields are not mass eigenstates but are actually a linear combination of mass eigenstates

$$|\nu_\alpha\rangle = \sum_i U^*_{\alpha i} |\nu_i\rangle \ , \tag{2.1}$$

where U is a unitary mixing matrix also called *Pontecorvo-Maki-Nakagawa-Sakata* (PMNS) matrix defined as

$$U = \begin{pmatrix} c_{12}c_{13} & s_{12}c_{13} & s_{13}e^{-i\delta} \\ -s_{12}c_{23} - c_{12}s_{23}s_{13}e^{i\delta} & c_{12}c_{23} - s_{12}s_{23}s_{13}e^{i\delta} & s_{23}c_{13} \\ s_{12}s_{23} - c_{12}c_{23}s_{13}e^{i\delta} & -c_{12}s_{23} - s_{12}c_{23}s_{13}e^{i\delta} & c_{23}c_{13} \end{pmatrix} , \tag{2.2}$$

where $c_{ij} = \cos\theta_{ij}$ and $s_{ij} = \sin\theta_{ij}$, while the θ_{ij} (mixing angle) and δ (CP phase) are parameters of Standard Model and as such are determined experimentally.

Neutrinos interact in CC interactions as flavour states, but propagate through space as mass eigenstates, usually denoted as ν_1, ν_2 and ν_3. Since the three mass eigenstates do not have the same mass, interference of these masses generates neutrino oscillations.

2.2 Neutrino oscillations in vacuum

Neutrino oscillations as a phenomenon were first proposed by Pontecorvo in the 1950s. It came as an analogy to the $K^0 - \overline{K}^0$ oscillations. But as the phenomenon required for neutrinos to have mass it was not taken seriously until first evidence of neutrino oscillations were observed which created a problem known as *Solar neutrino problem*. The problem originates from an experiment done in the late 1960s by Ray Davis and John N. Bahcall known as the Homestake Experiment. They measured the flux of neutrinos produced in the Sun and observed only one-third of the expected flux [4]. It was not until 1998 that the additional compelling evidence of neutrino oscillations were observed by Super Kamiokande (Super-K) project [5] and in 2001 by Sudbury Neutrino Observatory (SNO) [6] which resulted in a 2015 Nobel Prize in Physics to Takaaki Kajita (Super-K) and Arthur McDonald (SNO).

To describe these oscillations mathematically one starts with a newly formed flavour state which was created in a CC interaction [2],

$$|\nu_\alpha\rangle = \sum_k U^*_{\alpha k} |\nu_k\rangle \ .$$

Describing this newly formed neutrino at a later time T (corresponding to another CC interaction), at distance L, is done by applying space-time translation operator to the original state

$$|\nu_\alpha(L,T)\rangle = \sum_k U^*_{\alpha k} e^{-iE_kT+ip_kL} |\nu_k\rangle \ , \tag{2.3}$$

where the E_k is the energy and p_k is the momentum of the massive neutrino eigenstate ν_k. Using the unitarity property (2.4) of the mixing matrix U, the massive eigenstate can be expressed as a linear combination of flavour states (2.5),

$$\sum_\alpha U^*_{\alpha k} U_{\alpha j} = \delta_{jk} \ , \tag{2.4}$$

$$|\nu_k\rangle = \sum_\alpha U_{\alpha k} |\nu_\alpha\rangle \ . \tag{2.5}$$

Substituting this into (2.3) one gets

$$|\nu_\alpha(L,T)\rangle = \sum_\rho \left(\sum_k U^*_{\alpha k} e^{-iE_kT+ip_kL} U_{\rho k} \right) |\nu_\rho\rangle \ . \tag{2.6}$$

To find the probability amplitude of state $|\nu_\alpha(L,T)\rangle$ interacting as a flavour state $|\nu_\beta\rangle$ requires multiplying the equation from the left with $\langle\nu_\beta|$. Using the fact that $\langle\nu_\beta|\nu_\rho\rangle = \delta_{\beta\rho}$ gives

$$\langle\nu_\beta|\nu_\alpha(L,T)\rangle = \sum_k U^*_{\alpha k} e^{-iE_kT+ip_kL} U_{\beta k} \ , \tag{2.7}$$

Taking the absolute value of above expression gives the probability of oscillation

$$P_{\nu_\alpha\to\nu_\beta} = |\ \langle\nu_\beta|\nu_\alpha(L,T)\rangle\ |^2 = \left| \sum_k U^*_{\alpha k} e^{-iE_kT+ip_kL} U_{\beta k} \right|^2 \ . \tag{2.8}$$

As one can see, the probability of oscillation depends on the time of propagation of the neutrino. This is not extremely useful as in the experiments it is sometimes difficult to measure time of propagation. The usual approach would be to express time as distance traveled. For ultrarelativistic neutrinos, $T = L$ ($c = 1$). Using this, following approximations can be made

$$E_kT - p_kL = (E_k - p_k)L = \frac{E_k^2 - p_k^2}{E_k + p_k}L = \frac{m_k^2}{E_k + p_k}L \approx \frac{m_k^2}{2E}L \ , \tag{2.9}$$

where E is the kinetic energy of the neutrino which is taken to be total energy in the ultrarelativistic limit. With these approximations, probability takes the following form

$$P_{\nu_\alpha\to\nu_\beta} = \left| \sum_k U^*_{\alpha k} e^{-i\frac{m_{kj}^2}{2E}L} U_{\beta k} \right|^2 = \sum_{k,j} U^*_{\alpha k} U_{\beta k} U_{\alpha j} U^*_{\beta j} e^{-i\frac{\Delta m_{kj}^2}{2E}L} \ , \tag{2.10}$$

where $\Delta m^2_{kj} = m^2_k - m^2_j$. This now can be rewritten by splitting the sum into three parts ($k = j$, $k < j$, and $k > j$) to get the form

$$P_{\nu_\alpha\to\nu_\beta} = \sum_k \left|U^2_{\alpha k}\right| \left|U^2_{\beta k}\right| + 2\mathfrak{Re} \left[\sum_{k>j} U^*_{\alpha k} U_{\beta k} U_{\alpha j} U^*_{\beta j} e^{-i\frac{\Delta m_{kj}^2}{2E}L} \right] \ . \tag{2.11}$$

To make this equation easy to work with, some modifications are in order. First, one takes the unitarity relation (2.4) and square it to get

$$\begin{aligned}
\sum_{k,j} U^*_{\alpha k} U_{\beta k} U_{\alpha j} U^*_{\beta j} &= \delta_{\alpha\beta} \\
\sum_k |U_{\alpha k}|^2 \left|U_{\beta k}\right|^2 + \sum_{k>j} U^*_{\alpha k} U_{\beta k} U_{\alpha j} U^*_{\beta j} + \sum_{k<j} U^*_{\alpha k} U_{\beta k} U_{\alpha j} U^*_{\beta j} &= \delta_{\alpha\beta} \\
\sum_k |U_{\alpha k}|^2 \left|U_{\beta k}\right|^2 + \sum_{k>j} U^*_{\alpha k} U_{\beta k} U_{\alpha j} U^*_{\beta j} + \sum_{k>j} U^*_{\alpha j} U_{\beta j} U_{\alpha k} U^*_{\beta k} &= \delta_{\alpha\beta} \\
\sum_k |U_{\alpha k}|^2 \left|U_{\beta k}\right|^2 + 2\sum_{k>j} \mathfrak{Re}\left[U^*_{\alpha k} U_{\beta k} U_{\alpha j} U^*_{\beta j}\right] &= \delta_{\alpha\beta} \ , \qquad (2.12)
\end{aligned}$$

which then finally gives

$$\sum_k |U_{\alpha k}|^2 \left|U_{\beta k}\right|^2 = \delta_{\alpha\beta} - 2\sum_{k>j} \mathfrak{Re}\left[U^*_{\alpha k} U_{\beta k} U_{\alpha j} U^*_{\beta j}\right] \ . \qquad (2.13)$$

Inserting this into (2.11) one gets

$$P_{\nu_\alpha \to \nu_\beta} = \delta_{\alpha\beta} - 2\sum_{k>j} \mathfrak{Re}\left[U^*_{\alpha k} U_{\beta k} U_{\alpha j} U^*_{\beta j}\right] + 2\mathfrak{Re}\left[\sum_{k>j} U^*_{\alpha k} U_{\beta k} U_{\alpha j} U^*_{\beta j} e^{-i\frac{\Delta m^2_{kj}}{2E}L}\right] \ , \qquad (2.14)$$

which can be finally written as,

$$\begin{aligned}
P_{\nu_\alpha \to \nu_\beta} = \delta_{\alpha\beta} &- 4\sum_{k>j} \mathfrak{Re}\left[U^*_{\alpha k} U_{\beta k} U_{\alpha j} U^*_{\beta j}\right] \sin^2\left(\frac{\Delta m^2_{kj}}{4E} L\right) \\
&+ 2\sum_{k>j} \mathfrak{Im}\left[U^*_{\alpha k} U_{\beta k} U_{\alpha j} U^*_{\beta j}\right] \sin\left(\frac{\Delta m^2_{kj}}{2E} L\right) \ , \qquad (2.15)
\end{aligned}$$

where $\mathfrak{Re}(z_1 + z_2) = \mathfrak{Re}(z_1) + \mathfrak{Re}(z_2)$, $\mathfrak{Re}(i \times z) = -\mathfrak{Im}(z)$ and basic trigonometric identities such as $e^{ix} = \cos x + i \sin x$, $\cos 2x = \cos^2 x - \sin^2 x$ and $1 = \cos^2 x + \sin^2 x$ were used.

This is the final oscillation probability formula that will be used for the rest of the thesis. Notice that only the neutrino case has been studied while ignoring the antineutrino case. It is because the derivation is a complete analogy with small differences at the starting point. For antineutrinos the starting state (created in a CC interaction) is

$$|\overline{\nu}_\alpha\rangle = \sum_k U_{\alpha k} |\overline{\nu}_k\rangle \ , \qquad (2.16)$$

which, with the same derivation as the neutrino case, leads to the probability

$$P_{\overline{\nu}_\alpha \to \overline{\nu}_\beta} = \delta_{\alpha\beta} \quad - \quad 4\sum_{k>j} \mathfrak{Re}\left[U^*_{\alpha k} U_{\beta k} U_{\alpha j} U^*_{\beta j}\right] \sin^2\left(\frac{\Delta m^2_{kj}}{4E} L\right) \tag{2.17}$$

$$- \quad 2\sum_{k>j} \mathfrak{Im}\left[U^*_{\alpha k} U_{\beta k} U_{\alpha j} U^*_{\beta j}\right] \sin\left(\frac{\Delta m^2_{kj}}{2E} L\right) \ . \tag{2.18}$$

As can be seen in the equation above, the difference is only in the sign in front of the last term.

2.3 Neutrino oscillations in matter

Until now only neutrino oscillations in vacuum have been considered, but today's accelerator neutrino experiments are not done in the vacuum of space but underground where matter is present. The study of how the presence of matter affects the neutrino oscillations is required. Mathematically, this is done by adding the effective matter potential to the original vacuum Hamiltonian.

$$\mathcal{H} = \mathcal{H}_0 + \mathcal{H}_{eff} \ , \tag{2.19}$$

where

$$\begin{aligned} \mathcal{H}_0 \left|\nu_k\right\rangle &= E_k \left|\nu_k\right\rangle \\ \mathcal{H}_{eff} \left|\nu_\alpha\right\rangle &= V_\alpha \left|\nu_\alpha\right\rangle \ . \end{aligned} \tag{2.20}$$

This newly added potential is a result of the coherent forward elastic scattering of neutrinos on electrons (CC), protons (CC) and neutrons (NC) which can be seen in Fig. 2.1.

As can be seen, only electron neutrinos contribute to CC interactions in this particular scenario, while NC interactions include all three. The potential V_α can be split into two parts $V_\alpha = V^{CC}_\alpha + V^{NC}$, where contributions from CC and NC interactions are separate. While the V^{NC} is not zero it does not contribute to the neutrino oscillations as the constants phase it produces is added to all flavours equally. With this in mind, only V^{CC}_α will be taken into the account which has the form (for detailed derivation of V^{CC}_α refer to [2])

$$V^{CC}_\alpha = V\delta_{\alpha e} = \sqrt{2} G_F N_e \delta_{\alpha e} \ , \tag{2.21}$$

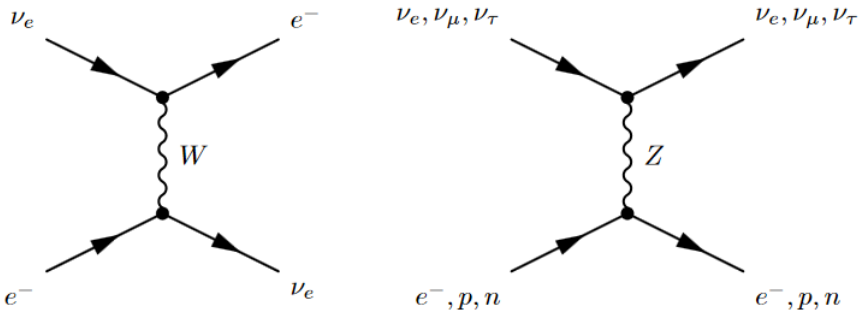

Figure 2.1: Feynman diagrams of the coherent forward elastic scattering processes that generate the CC potential V_α^{CC} through W exchange and the NC potential V^{NC} through Z exchange. Taken from [2].

where G_F is the Fermi constant and N_e is the concentration of electrons in the volume of matter neutrinos propagate through.

Now that the potential has been defined, one can start to derive the neutrino oscillations in matter. This begins with the equation of evolution for the starting flavour state

$$i\frac{\mathrm{d}}{\mathrm{dt}}\left|\nu_\alpha(t)\right\rangle = \mathcal{H}\left|\nu_\alpha(t)\right\rangle \ . \tag{2.22}$$

Applying (2.19) gives

$$i\frac{\mathrm{d}}{\mathrm{dt}}\left|\nu_\alpha(t)\right\rangle = \mathcal{H}_0\left|\nu_\alpha(t)\right\rangle + \mathcal{H}_1\left|\nu_\alpha(t)\right\rangle \ . \tag{2.23}$$

Now, one can notice that in (2.20), $\mathcal{H}_0$ acts on mass states while $\mathcal{H}_1$ acts on flavour states. This means, that the first term on the right-hand side of (2.23) needs to be changed into the mass basis using (2.1)

$$i\frac{\mathrm{d}}{\mathrm{dt}}\left|\nu_\alpha(t)\right\rangle = \sum_k E_k U_{\alpha k}^*\left|\nu_k(t)\right\rangle + V_\alpha\left|\nu_\alpha(t)\right\rangle \ . \tag{2.24}$$

Returning the first term to flavour basis gives[1]

$$i\frac{\mathrm{d}}{\mathrm{dt}}\left|\nu_\alpha(t)\right\rangle = \sum_k\sum_\eta E_k U_{\alpha k}^* U_{\eta k}\left|\nu_\eta(t)\right\rangle + V_\alpha\left|\nu_\alpha(t)\right\rangle \ . \tag{2.25}$$

Using $\sum_\eta V_\eta \delta_{\eta\alpha} = V_\alpha$ and (2.21), equation (2.25) becomes

$$i\frac{\mathrm{d}}{\mathrm{dt}}\left|\nu_\alpha(t)\right\rangle = \sum_\eta\left[\sum_k E_k U_{\alpha k}^* U_{\eta k} + V\delta_{\eta e}\delta_{\eta\alpha}\right]\left|\nu_\eta(t)\right\rangle \ . \tag{2.26}$$

[1] All sums marked with Greek letters go over the neutrino flavour states (e, μ, τ) while Latin letters indicate sum over mass states $(1, 2, 3)$.

Now, as before, the goal is to find probability amplitude of starting neutrino state $|\nu_\alpha\rangle$ interacting at a later time as another state $|\nu_\beta\rangle$,

$$i\frac{\mathrm{d}}{\mathrm{dt}}\langle\nu_\beta|\nu_\alpha(t)\rangle = \sum_\eta \left[\sum_k E_k U^*_{\alpha k} U_{\eta k} + V\delta_{\eta e}\delta_{\eta\alpha}\right]\langle\nu_\beta|\nu_\eta(t)\rangle \ . \tag{2.27}$$

To find the squared mass differences in matter, one needs to first change to vacuum mass eigenbasis. This is done by first multiplying equation (2.27) from the left by $\sum_\alpha \sum_\beta U_{\alpha i} U^*_{\beta j}$ and using (2.5),

$$i\frac{\mathrm{d}}{\mathrm{dt}}\langle\nu_j|\nu_i(t)\rangle = \sum_{\eta,\alpha,\beta} \left[\sum_k E_k U^*_{\alpha k} U_{\eta k} + V\delta_{\eta e}\delta_{\eta\alpha}\right] U_{\alpha i} U^*_{\beta j}\langle\nu_\beta|\nu_\eta(t)\rangle \ . \tag{2.28}$$

Now, applying equation (2.1) again on the right-hand side, one gets

$$i\frac{\mathrm{d}}{\mathrm{dt}}\langle\nu_j|\nu_i(t)\rangle = \sum_{\eta,\alpha,\beta}\sum_{m,n} \left[\sum_k E_k U^*_{\alpha k} U_{\eta k} + V\delta_{\eta e}\delta_{\eta\alpha}\right] U_{\alpha i} U^*_{\beta j} U_{\beta m} U^*_{\eta n}\langle\nu_m|\nu_n(t)\rangle \ . \tag{2.29}$$

Multiplying the bracket for clarity gives

$$\begin{aligned} i\frac{\mathrm{d}}{\mathrm{dt}}\langle\nu_j|\nu_i(t)\rangle = \quad & \sum_{\eta,\alpha,\beta}\sum_{m,n,k} E_k U^*_{\alpha k} U_{\eta k} U_{\alpha i} U^*_{\beta j} U_{\beta m} U^*_{\eta n}\langle\nu_m|\nu_n(t)\rangle + \\ & \sum_{\eta,\alpha,\beta}\sum_{m,n} V\delta_{\eta e}\delta_{\eta\alpha} U_{\alpha i} U^*_{\beta j} U_{\beta m} U^*_{\eta n}\langle\nu_m|\nu_n(t)\rangle \ . \end{aligned} \tag{2.30}$$

Using unitarity (2.4), the first term gives

$$\begin{aligned} \sum_{\eta,\alpha,\beta}\sum_{m,n,k} E_k U^*_{\alpha k} U_{\eta k} U_{\alpha i} U^*_{\beta j} U_{\beta m} U^*_{\eta n}\langle\nu_m|\nu_n(t)\rangle &= \sum_{m,n,k} E_k \delta_{ki}\delta_{jm}\delta_{kn}\langle\nu_m|\nu_n(t)\rangle \\ &= \sum_{m,n} E_i \delta_{in}\delta_{jm}\langle\nu_m|\nu_n(t)\rangle \\ &= \sum_n E_i\delta_{in}\langle\nu_j|\nu_n(t)\rangle \ , \end{aligned} \tag{2.31}$$

while the second term becomes

$$\begin{aligned} \sum_{\eta,\alpha,\beta}\sum_{m,n} V\delta_{\eta e}\delta_{\eta\alpha} U_{\alpha i} U^*_{\beta j} U_{\beta m} U^*_{\eta n}\langle\nu_m|\nu_n(t)\rangle &= \sum_{m,n} V\delta_{jm} U_{ei} U^*_{en}\langle\nu_m|\nu_n(t)\rangle \\ &= \sum_n V U_{ei} U^*_{en}\langle\nu_j|\nu_n(t)\rangle \ . \end{aligned} \tag{2.32}$$

Putting both terms back together, one finally gets

$$i\frac{\mathrm{d}}{\mathrm{dt}}\langle\nu_j|\nu_i(t)\rangle = \sum_n \left(E_i\delta_{in} + V U_{ei} U^*_{en}\right)\langle\nu_j|\nu_n(t)\rangle \ . \tag{2.33}$$

Here the approximations for ultrarelativistic neutrinos, introduced in (2.9), can be used

$$i\frac{\mathrm{d}}{\mathrm{dt}}\left\langle \nu_j|\nu_i(t)\right\rangle = \frac{1}{2E}\sum_n \left(m_i^2\delta_{in} + DU_{ei}U_{en}^*\right)\left\langle \nu_j|\nu_n(t)\right\rangle \ , \tag{2.34}$$

where now $D = 2\sqrt{2}G_F N_e E$. Using the matrix U as defined in (2.2) the equation can be written in matrix form

$$i\frac{\mathrm{d}}{\mathrm{dt}}\begin{pmatrix}\psi_{1j}\\ \psi_{2j}\\ \psi_{3j}\end{pmatrix} = \frac{1}{2E}\begin{pmatrix} m_1^2 + Dc_{12}^2c_{13}^2 & Dc_{12}s_{12}c_{13}^2 & Dc_{12}c_{13}s_{13}e^{i\delta}\\ Dc_{12}s_{12}c_{13}^2 & m_2^2 + Ds_{12}^2c_{13}^2 & Ds_{12}s_{13}c_{13}e^{i\delta}\\ Dc_{12}c_{13}s_{13}e^{-i\delta} & Ds_{12}c_{13}s_{13}e^{-i\delta} & m_3^2 + Ds_{13}^2\end{pmatrix}\begin{pmatrix}\psi_{1j}\\ \psi_{2j}\\ \psi_{3j}\end{pmatrix}, \tag{2.35}$$

where $\psi_{ij} = \langle\nu_j|\nu_i(t)\rangle$.

This is the evolution of initial neutrino mass eigenstates in matter depicted in vacuum eigenbasis. However, the desired result is the neutrino mass eigenstates in matter, depicted in matter eigenbasis, as then one can easily read off diagonal terms of the matrix which correspond to mass eigenvalues in matter eigenbasis. To do this, one needs to diagonalize the matrix in (2.35). Fortunately, this can be done by finding the eigenvalues of the matrix as they correspond to the values on the diagonal in diagonalized form of the matrix.

To do this, one writes down the characteristic polynomial which is a cubic equation

$$\begin{aligned} &X^3 - (m_1^2 + m_2^2 + m_3^2 + D)X^2 \\ &+ \left[m_1^2m_2^2 + m_2^2m_3^2 + m_1^2m_3^2 + D(m_3^2c_{13}^2 + m_2^2(c_{13}^2c_{12}^2 + s_{13}^2) + m_1^2(c_{13}^2s_{12}^2 + s_{13}^2))\right]X \\ &- \left[m_1^2m_2^2m_3^2 + D(m_3^2m_2^2c_{13}^2c_{12}^2 + m_3^2m_1^2c_{13}^2s_{12}^2 + m_2^2m_1^2s_{13}^2)\right] = 0\ . \end{aligned} \tag{2.36}$$

Solutions for this polynomial have been taken from [7] and they are three eigenvalues which correspond to squared masses of matter mass eigenstates.

$$M_1^2 = m_1^2 + \frac{A}{3} - \frac{1}{3}\sqrt{A^2 - 3B}S - \frac{\sqrt{3}}{3}\sqrt{A^2 - 3B}\sqrt{1 - S^2} \tag{2.37}$$

$$M_2^2 = m_1^2 + \frac{A}{3} - \frac{1}{3}\sqrt{A^2 - 3B}S + \frac{\sqrt{3}}{3}\sqrt{A^2 - 3B}\sqrt{1 - S^2} \tag{2.38}$$

$$M_3^2 = m_1^2 + \frac{A}{3} + \frac{2}{3}\sqrt{A^2 - 3B}S\ , \tag{2.39}$$

here the abbreviations used are

$$A = \Delta m^2_{21} + \Delta m^2_{31} + D \tag{2.40}$$

$$B = \Delta m^2_{31}\Delta m^2_{21} + D[\Delta m^2_{31}c^2_{13} + \Delta m^2_{21}(c^2_{13}c^2_{12} + s^2_{13})] \tag{2.41}$$

$$C = D\Delta m^2_{31}\Delta m^2_{21}c^2_{13}c^2_{12} \tag{2.42}$$

$$S = \cos\left[\frac{1}{3}\arccos\left(\frac{2A^3 - 9AB + 27C}{2\sqrt{A^2 - 3B}^3}\right)\right] . \tag{2.43}$$

As one is interested in squared mass differences, one has

$$\Delta M^2_{21} = \frac{2\sqrt{3}}{3}\sqrt{A^2 - 3B}\sqrt{1 - S^2} \tag{2.44}$$

$$\Delta M^2_{31} = \sqrt{A^2 - 3B}S + \frac{\sqrt{3}}{3}\sqrt{A^2 - 3B}\sqrt{1 - S^2} \tag{2.45}$$

$$\Delta M^2_{32} = \sqrt{A^2 - 3B}S - \frac{\sqrt{3}}{3}\sqrt{A^2 - 3B}\sqrt{1 - S^2} . \tag{2.46}$$

Here the key takeaway is that these squared mass differences in matter depend only on the vacuum squared mass differences and vacuum mixing angles, which is fortunate as these parameters are the ones that are measured in experiments.

As the eigenbasis has been changed (from vacuum to matter), mixing matrix parameters also changed in this new basis. To get these parameters one firstly needs to find transformation matrix W defined as

$$W^{-1}\begin{pmatrix} m^2_1 + Dc^2_{12}c^2_{13} & Dc_{12}s_{12}c^2_{13} & Dc_{12}c_{13}s_{13}e^{i\delta} \\ Dc_{12}s_{12}c^2_{13} & m^2_2 + Ds^2_{12}c^2_{13} & Ds_{12}s_{13}c_{13}e^{i\delta} \\ Dc_{12}c_{13}s_{13}e^{-i\delta} & Ds_{12}c_{13}s_{13}e^{-i\delta} & m^2_3 + Ds^2_{13} \end{pmatrix} W = \begin{pmatrix} M^2_1 & 0 & 0 \\ 0 & M^2_2 & 0 \\ 0 & 0 & M^2_3 \end{pmatrix} . \tag{2.47}$$

One way of finding this W matrix is by using the fact that its columns are the eigenstates of corresponding eigenvalues in (2.37). W can be used to find the new mixing matrix V as

$$V = UW , \tag{2.48}$$

where V is now

$$\begin{pmatrix} |\nu_e\rangle \\ |\nu_\mu\rangle \\ |\nu_\tau\rangle \end{pmatrix} = V \begin{pmatrix} |\nu_{1m}\rangle \\ |\nu_{2m}\rangle \\ |\nu_{3m}\rangle \end{pmatrix} . \tag{2.49}$$

This process (for more details refer to [7]) results in following matter mixing angles

$$s_{12}^{m2} = \frac{-(M_2^4 - \alpha M_2^2 + \beta)\Delta M_{31}^2}{\Delta M_{32}^2(M_1^4 - \alpha M_1^2 + \beta) - \Delta M_{31}^2(M_2^4 - \alpha M_2^2 + \beta)} \quad (2.50)$$

$$s_{13}^{m2} = \frac{M_3^4 - \alpha M_3^2 + \beta}{\Delta M_{31}^2 \Delta M_{32}^2} \quad (2.51)$$

$$s_{23}^{m2} = \frac{E^2 s_{23}^2 + F^2 c_{23}^2 + 2EFc_{23}s_{23}c_\delta}{E^2 + F^2} \quad (2.52)$$

$$e^{-i\delta^m} = \frac{(E^2 e^{-i\delta} - F^2 e^{i\delta})s_{23}c_{23} + EF(c_{23}^2 - s_{23}^2)}{\sqrt{(E^2 s_{23}^2 + F^2 c_{23}^2 + 2EFc_{23}s_{23}c_\delta)(E^2 c_{23}^2 + F^2 s_{23}^2 - 2EFc_{23}s_{23}c_\delta)}} \,, \quad (2.53)$$

with following abbreviations

$$\alpha = m_3^2 c_{13}^2 + m_2^2(c_{13}^2 c_{12}^2 + s_{13}^2) + m_1^2(c_{13}^2 s_{12}^2 + s_{13}^2) \quad (2.54)$$

$$\beta = m_3^2 c_{13}^2(m_2^2 c_{12}^2 + m_1^2 s_{12}^2) + m_2^2 m_1^2 s_{13}^2 \quad (2.55)$$

$$E = [\Delta m_{31}^2(M_3^2 - m_1^2 - \Delta m_{21}^2) - \Delta m_{21}^2(M_3^2 - m_1^2 - \Delta m_{31}^2)s_{12}^2]c_{13}s_{13} \quad (2.56)$$

$$F = (M_3^2 - m_1^2 - \Delta m_{31}^2)\Delta m_{21}^2 c_{12}s_{12}c_{13} \,. \quad (2.57)$$

Although it seems there are dependencies on squared masses directly in (2.51) and (2.50), with a bit of arithmetic it can be shown they disappear

$$s_{13}^{m2} = \frac{K_3}{\Delta M_{31}^2 \Delta M_{32}^2} \quad (2.58)$$

$$s_{12}^{m2} = \frac{-K_2 \Delta M_{31}^2}{\Delta M_{32}^2 K_1 - \Delta M_{31}^2 K_3} \,, \quad (2.59)$$

where

$$K_1 = T_1^2 - \Delta m_{31}^2 c_{13}^2 T_1 - \Delta m_{31}^2 T_1(c_{13}^2 c_{12}^2 + s_{13}^2) + \Delta m_{31}^2 \Delta m_{21}^2 c_{12}^2 c_{13}^2 \quad (2.60)$$

$$K_2 = T_2^2 - \Delta m_{31}^2 c_{13}^2 T_2 - \Delta m_{31}^2 T_2(c_{13}^2 c_{12}^2 + s_{13}^2) + \Delta m_{31}^2 \Delta m_{21}^2 c_{12}^2 c_{13}^2 \quad (2.61)$$

$$K_3 = T_3^2 - \Delta m_{31}^2 c_{13}^2 T_3 - \Delta m_{31}^2 T_3(c_{13}^2 c_{12}^2 + s_{13}^2) + \Delta m_{31}^2 \Delta m_{21}^2 c_{12}^2 c_{13}^2 \quad (2.62)$$

$$T_1 = \frac{A}{3} - \frac{1}{3}\sqrt{A^2 - 3B}S - \frac{\sqrt{3}}{3}\sqrt{A^2 - 3B}\sqrt{1 - S^2} \quad (2.63)$$

$$T_2 = \frac{A}{3} - \frac{1}{3}\sqrt{A^2 - 3B}S + \frac{\sqrt{3}}{3}\sqrt{A^2 - 3B}\sqrt{1 - S^2} \quad (2.64)$$

$$T_3 = \frac{A}{3} + \frac{2}{3}\sqrt{A^2 - 3B}\sqrt{1 - S^2} \,. \quad (2.65)$$

From this its obvious that neutrino oscillations in matter also depend only on mass square differences in vacuum and vacuum mixing angles. On one side this is unfortunate as this means matter effects can not be used to measure the masses of neutrino mass eigenstates

directly, but it is also fortunate as it allows probability calculations without knowing the masses directly.

The only thing left is to write out the equation for probability of oscillation which is completely analogous to (2.15).

$$P_{\nu_\alpha \to \nu_\beta} = \delta_{\alpha\beta} \quad - \quad 4 \sum_{k>j} \mathfrak{Re}\left[V^*_{\alpha k} V_{\beta k} V_{\alpha j} V^*_{\beta j}\right] \sin^2\left(\frac{\Delta M^2_{kj}}{4E} L\right) \tag{2.66}$$

$$\pm \quad 2 \sum_{k>j} \mathfrak{Im}\left[V^*_{\alpha k} V_{\beta k} V_{\alpha j} V^*_{\beta j}\right] \sin\left(\frac{\Delta M^2_{kj}}{2E} L\right) \tag{2.67}$$

For antineutrino case, the constant D also changes a sign.

2.4 CP violation

Charge (C), Parity (P) and Time reversal (T) symmetries are discrete symmetries and as a result they do not have any conserved currents. C symmetry transforms a particle into its antiparticle, P changes signs of all spatial coordinates resulting in changing of helicity and T, as its name suggests, reverses process in question. When these symmetries are applied to the system simultaneously, we have what is known as CPT symmetry which is a symmetry for all local quantum field theories including SM.

All three symmetries by themselves are known to be violated [8] and, as CPT = 1, all the combinations of two symmetries are also known to be violated. Most interesting of these is CP symmetry (which transforms left handed neutrinos into right handed antineutrinos). Although CP violations are allowed in SM in different sectors including strong CP violation [9], the only confirmed case of CP violation, at the time of writing, is in the weak mixing of the quark sector [10].

Another possible CP violation is in the lepton sector. If CP symmetry is conserved, the following would be true

$$P_{\nu_\alpha \to \nu_\beta} = P_{\overline{\nu}_\alpha \to \overline{\nu}_\beta} \ . \tag{2.68}$$

Using this, a measure of CP asymmetry can be defined as

$$A^{\mathrm{CP}}_{\alpha\beta} = P_{\nu_\alpha \to \nu_\beta} - P_{\overline{\nu}_\alpha \to \overline{\nu}_\beta} \ . \tag{2.69}$$

If $A^{CP}_{\alpha\beta} = 0$, CP symmetry is conserved and vice versa. Inserting (2.15) and (2.17) into this (for matter effects probability the structure is the same, only different parameters are used) gives

$$A^{CP}_{\alpha\beta} = 4 \sum_{k>j} \mathfrak{Im} \left[U^*_{\alpha k} U_{\beta k} U_{\alpha j} U^*_{\beta j} \right] \sin \left(\frac{\Delta m^2_{kj}}{2E} L \right) \ . \tag{2.70}$$

It is evident from equation above that for $\alpha = \beta$ CP is not violated as the imaginary part vanishes. More precisely, CP violation can not be observed in disappearance channels.

Looking at the example of muon neutrino oscillating into electron neutrino, one has

$$\begin{aligned} A^{CP}_{\mu e} &= P_{\nu_\mu \to \nu_e} - P_{\overline{\nu}_\mu \to \overline{\nu}_e} \\ &= 4 \sin \delta_{CP} \, s_{23} \, c^2_{13} \, s_{12} \, c_{23} \, s_{13} \, c_{12} \left[\sin \phi_{31} - \sin \phi_{32} - \sin \phi_{21} \right] \ , \end{aligned} \tag{2.71}$$

where $\phi_{ij} = \frac{\Delta m^2_{ij}}{2E} L$. The constant term in front of the bracket in (2.71) is often called a Jarlskog invariant after Cecilia Jarlskog who first introduced it,

$$J = 4 \sin \delta_{CP} \, s_{23} \, c^2_{13} \, s_{12} \, c_{23} \, s_{13} \, c_{12} \ . \tag{2.72}$$

It is obvious from (2.71) that $A^{CP}_{\alpha\beta} = 0$ if any two masses are the same or any mixing angle is 0 or $\pi/2$ or that δ_{CP} is equal to 0 or π. Experimentally, mass differences are not 0, nor are any angles 0 or $\pi/2$ so the only way left is that the δ_{CP} is 0 or π. Because of this, δ_{CP} is known as the CP-violating phase and it is a measure of CP violation in neutrino oscillations.

2.5 CC and NC interactions

Neutrino interacts through weak interaction via *charged-current* (CC), *neutral-current* (NC) or a combination of the two.

CC interactions are defined as interactions mediated by charged massive vector fields $W^{\pm}$. Feynman diagrams of leptons coupling to the $W^{\pm}$ fields are shown in Fig. 2.2.

The vertex factor for this coupling is

$$\frac{-i g_w}{2\sqrt{2}} \gamma_\mu (1 - \gamma_5) \ , \tag{2.73}$$

where γ_i are the Dirac matrices and g_w is the coupling constant for the weak interaction. It is connected to the electric charge through the Weinberg angle

$$g_w = \frac{e}{\sin^2 \theta_w} \ . \tag{2.74}$$

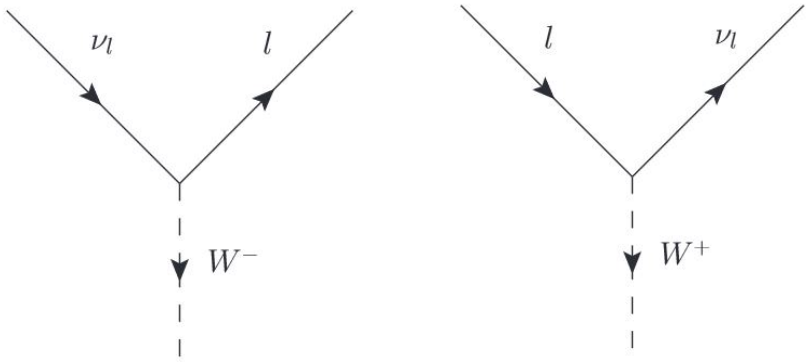

(a) (b)

Figure 2.2: Feynman diagrams of fermions coupling to W^+ and W^- bosons.

Further, the W propagator is

$$-i\frac{g_{\mu\nu} - \frac{q_\mu q_\nu}{M_W^2}}{q^2 - M_W^2} \,, \tag{2.75}$$

where q is the momentum of the propagator while the M_W is its mass. This can be approximated for low energies as

$$-i\frac{g_{\mu\nu}}{q^2 - M_W^2} \,. \tag{2.76}$$

NC interactions are defined as week interactions mediated by massive neutral vector field Z. Similar to W propagator, the Z propagator is

$$-i\frac{g_{\mu\nu} - \frac{q_\mu q_\nu}{M_Z^2}}{q^2 - M_Z^2} \,. \tag{2.77}$$

Vertex for neutrino coupling to Z boson is shown on Fig. 2.3 and the vertex factor is

$$\frac{-ig_w}{2}\gamma_\mu(c_V - c_A\gamma_5) \,, \tag{2.78}$$

where c_V is the vector current coupling constant while c_A is the axial current coupling constant. Their value depends on the type of a fermion. For all neutrinos both constants are $\frac{1}{2}$, while for charged leptons (electrons, muons and taus)

$$c_V = -\frac{1}{2} + 2\sin^2\theta_W \tag{2.79}$$

$$c_A = -\frac{1}{2} \,. \tag{2.80}$$

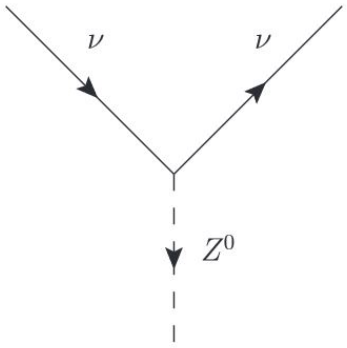

Figure 2.3: Feynman diagram of a neutrino coupling to Z boson

Neutrino interactions with matter differ with neutrino energy [11]. At lower energies at around 10 MeV, like such achieved in the Sun or nuclear reactors, neutrinos interact with entire nucleons in interactions such as inverse beta-decay of the proton

$$\overline{\nu}_e + p \longrightarrow e^+ + n \ . \tag{2.81}$$

Another possibility is the elastic scattering on electrons

$$\nu_e + e^- \longrightarrow \nu_e + e^- \ . \tag{2.82}$$

On the other hand, at higher energies, there are more types of interactions for neutrinos. First one is the elastic or quasi-elastic (QES) scattering, where a neutrino elastically scatters off a nucleon, liberating the said nucleon or multiple nucelons of the target. QES is referred to the CC interactions, while elastic is referred to NC interactions. Furthermore, neutrinos can interact with a nucleon and excite it to a resonance state after which it can decay into a final mesonic state, this interaction is known as resonant scattering (RES). At higher energies there is also deep inelastic scattering (DIS) of neutrinos. This is an interaction where a neutrino has enough energy to probe a nucleon and interact directly with a constituent of the said nucleon i.e. quark. Such scatterings are responsible for hadronic showers which are a good way of identifying the process. Note that the boundary between DIS and RES is not clearly defined.

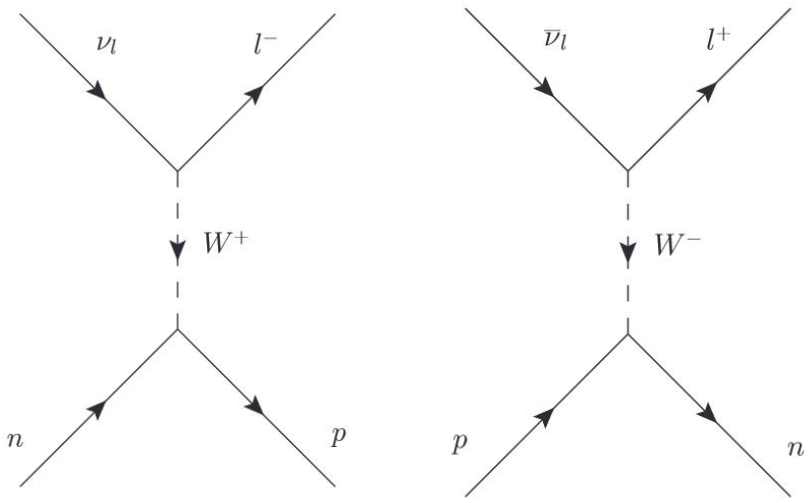

(a) (b)

Figure 2.4: Feynman diagrams of quasi-elastic neutrino scattering

3 ESSνSB

European Spallation Source Neutrino Super Beam (ESSνSB) [12] is a design study for an experiment to measure CP violation in leptonic sector by observing neutrino oscillations [13]. Method of observing this CP violation is to determine the difference between probabilities of neutrino and antineutrino oscillation

$$P_{\nu_\mu \to \nu_e} \neq P_{\bar{\nu}_\mu \to \bar{\nu}_e} \ . \tag{3.1}$$

This difference can be observed at the first or second oscillation maximum. However, the second oscillation maximum is giving a much better sensitivity to δ_{CP} than the first oscillation maximum, as can be seen on Fig. 4.4. For this reason, ESSνSB project has chosen to observe the neutrino oscillations at the second oscillation maximum.

3.1 Neutrino Beam production

The European Spallation Source facility currently under construction in Lund, Sweden will produce a beam of 2 GeV kinetic energy protons using 5 MW linac which will operate at a rate of 14 Hz. This will make it the most powerful proton accelerator in the world. Additionally, an upgrade of the accelerator is being planned to produce protons of 2.5 GeV kinetic energy. Accumulator ring will be used to shorten the pulses to reduce

the background coming from the atmospheric neutrinos [14]. Each proton pulse will be further split into four smaller pulses which will then impact the target. At the target, proton collision will happen, and the particles that come out of these collisions will be mostly pions. Pions will be focused by the magnetic horn and will then decay in the decay tunnel into leptons, almost exclusively into the (anti)muon and muon (anti)neutrino pair. Changing the polarity of the magnetic horn, one can choose which pions (negative or positive) to focus depending if the neutrino or antineutrino beam is wanted. Neutrino beam created by this process will be aimed at near and far detectors. Near detectors will be close to the source to ensure no neutrino oscillation is happening while far detectors will be placed farther where the neutrino oscillation will reach their second maximum.

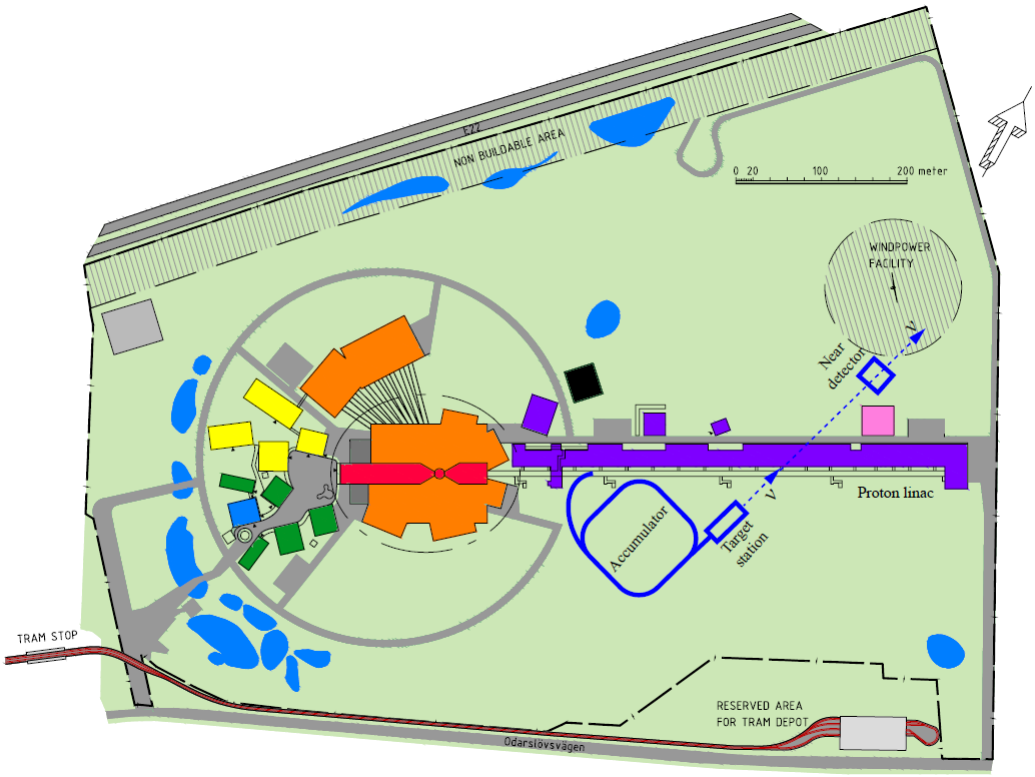

Figure 3.1: The ESS neutron and neutrino (in blue) facilities. Taken from [14].

3.2 Near Detectors

A group of near detectors will be placed at 250 m from the neutrino source. It will consist of 500 t water Cherenkov detector (NearWatCh), $\sim$ 1 t Super Fine-Grain Scintillation detector (SFGD) and an emulsion detector with a water target [15]. The main task of

near detectors is to measure neutrino flux and neutrino-water cross-sections. In the case of ESSνSB and sub-GeV energies it will deal with, measuring cross-section is extremely important as the current measurement of the sub-GeV cross-sections for neutrinos are extremely limited (see Fig. 51.1 in [16]). Measuring the neutrino flux will lower systematic uncertainties of the flux at the far detectors making measurements more precise.

NearWatCh will be the main detector, and its statistics will be used to determine the flux and cross-sections. As the name suggests it will use Cherenkov radiation as the detection method. After the interaction of a neutrino with the target at the detector, a charged lepton will be produced that will have a speed greater than that of light in the same medium. Such leptons then produce the Cherenkov light which is collected by the detector using photomultiplier tubes. Using Cherenkov light one can reconstruct the original path and energy of the charged lepton.

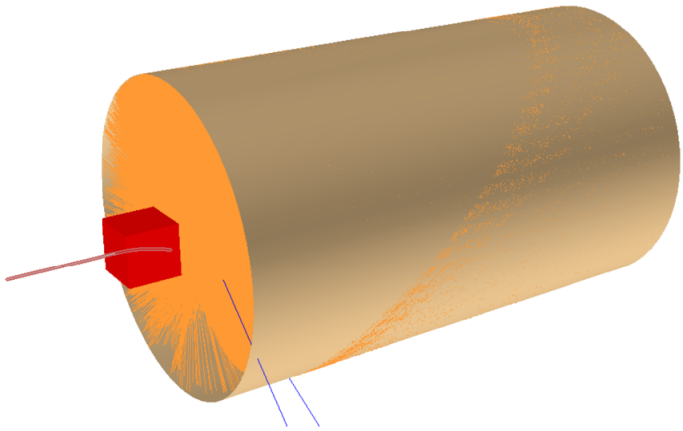

Figure 3.2: Simulation of the near detector hall. A muon (orange track) is passing both through the SFGD detector (red cube) and the water Cherenkov detector immediately downstream. Taken from [13].

3.3 Far Water Cherenkov Detectors

Far detectors will consist of two identical water Cherenkov detectors (FarWatCh). Location of the FarWatCh is still under consideration between two candidate sites. One at Zinkgruvan mine which is located 360 km from the neutrino source and the other is Garpenberg mine located 540 km from the neutrino source[2]. Total fiducial target mass

[2] For this thesis, calculations will be done assuming the Garpenberg location at 540 km distance from neutrino source (unless specified otherwise).

of the FarWatCh will be 538 kt. FarWatCh will use the same detection method as NearWatCh.

4 Expected number of neutrino interactions

Although the main focus of this thesis is calculating the expected number of interactions in the far detectors of the ESSνSB project, expected number of interactions for near detectors is also presented. The only difference is that for near detectors, neutrino oscillations can be neglected.

Expected number of neutrino interactions is important as it gives an upper limit on the statistics of the experiment, depending on the detector specifications. Using this, one can see if the goal of the experiment, in this case observing the CP violation, can be achieved. In following calculations, efficiency and geometry of the detector are not taken into the account. All calculations and plots have been done using programming languages C++ and ROOT [17].

There are two quantities that are important for calculating the expected number of interactions. One is the flux of neutrinos defined as number of neutrinos N passing through unit area A in unit time t

$$F(E) = \frac{1}{A}\frac{\mathrm{d}^2 N}{\mathrm{d}E\,\mathrm{d}t} \ . \tag{4.1}$$

The other is the interaction cross section which is a measure of probability of particle interacting with another particle. Both these quantities are related to the number of expected interactions as

$$\frac{\mathrm{d}N}{\mathrm{d}t} = F \times \sigma \ . \tag{4.2}$$

Integrating over time and having more than one target particle while also having a flux of neutrinos which is not monoenergetic expands this expression. General equation (in this case) for calculating the expected number of interactions per target per time is

$$\frac{N}{N_\mathrm{t} T} = \int_{E_1}^{E_2} F(E)\sigma(E)\mathrm{d}E \ , \tag{4.3}$$

where N_t is the number of targets (commonly atoms and molecules), T is time of observation, $\sigma(E)$ is the cross section of the incoming particle with the target and $F(E)$ is the incoming flux of neutrinos at the target location.

4.1 Neutrino Flux

Neutrino flux used in these calculations has been provided by ESSνSB project. Flux was provided in a histogram format with bin width of 0.02 GeV measured at a distance of 100 km from the source in the energy range of $0.04 - 2.0$ GeV. Units in which flux is given are

$$[F] = \left[\frac{N}{\mathrm{m}^2 \times 0.02\,\mathrm{GeV} \times 200\,\mathrm{days}}\right] , \tag{4.4}$$

where N is the number of neutrinos. Fluxes used can be seen in Fig. 4.1 and Fig. 4.2.

As expected from the design of the experiment, ν_μ flux is the biggest in positive polarity while $\bar{\nu}_\mu$ is the biggest flux in negative polarity. This is desirable as these are the neutrinos that will oscillate into ν_e and $\bar{\nu}_e$ which are the channels that are considered to be a "signal". For the ease of use in the code it is desirable to scale the flux to 1 km and to have a unit of

$$[F] = \left[\frac{N}{\mathrm{cm}^2 \times \mathrm{GeV} \times \mathrm{p\,o\,t}}\right] \tag{4.5}$$

where p.o.t. means *protons on target*. This way it is much easier to manipulate this flux for any calculation wanted.

As the flux has inverse square relation with distance

$$F \propto \frac{1}{r^2}, \tag{4.6}$$

it is scaled to 1 km by multiplying each bin by 100^2. To change the unit of the flux from (4.4) to (4.5) one has to multiply each bin by normalization constant $C = \frac{1}{100^2} \times 0.02 \times 2.16 \times 10^{23}$. With this, to get flux at any distance, just divide each bin by the distance (in kilometers) squared.

4.2 Cross section

Since the detectors are using water (H_2O) as a medium, cross section of the water molecule is needed. Using GENIE [18, 19, 20], it is possible to get cross sections of individual atoms. For water, these atoms are oxygen and hydrogen. GENIE cross sections include

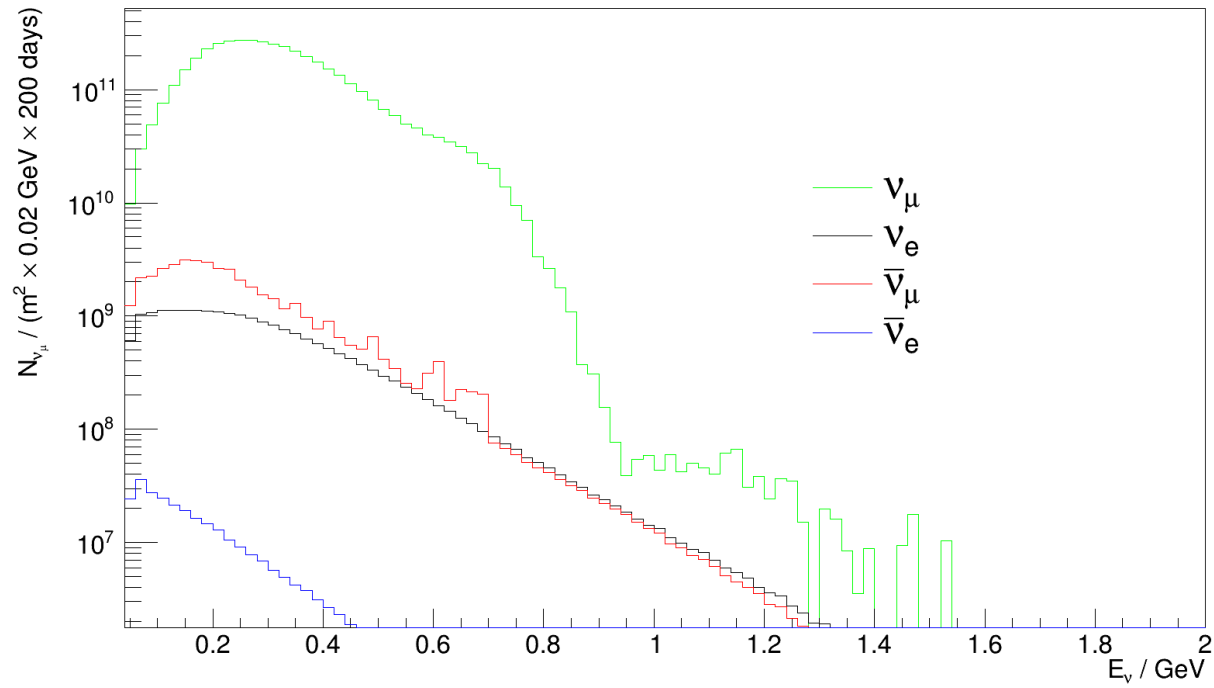

(a)

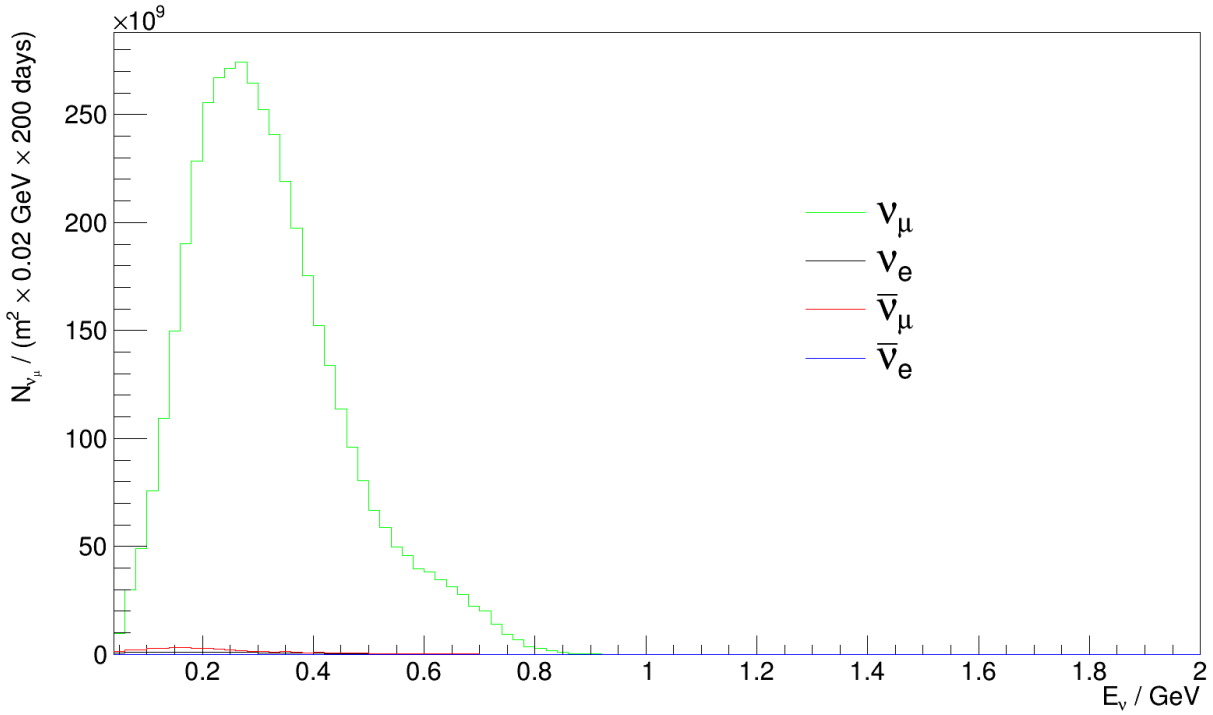

(b)

Figure 4.1: Neutrino fluxes as functions of energy produced in positive polarity mode at 100 km from the source in 200 days. Top figure is logarithmic scale.

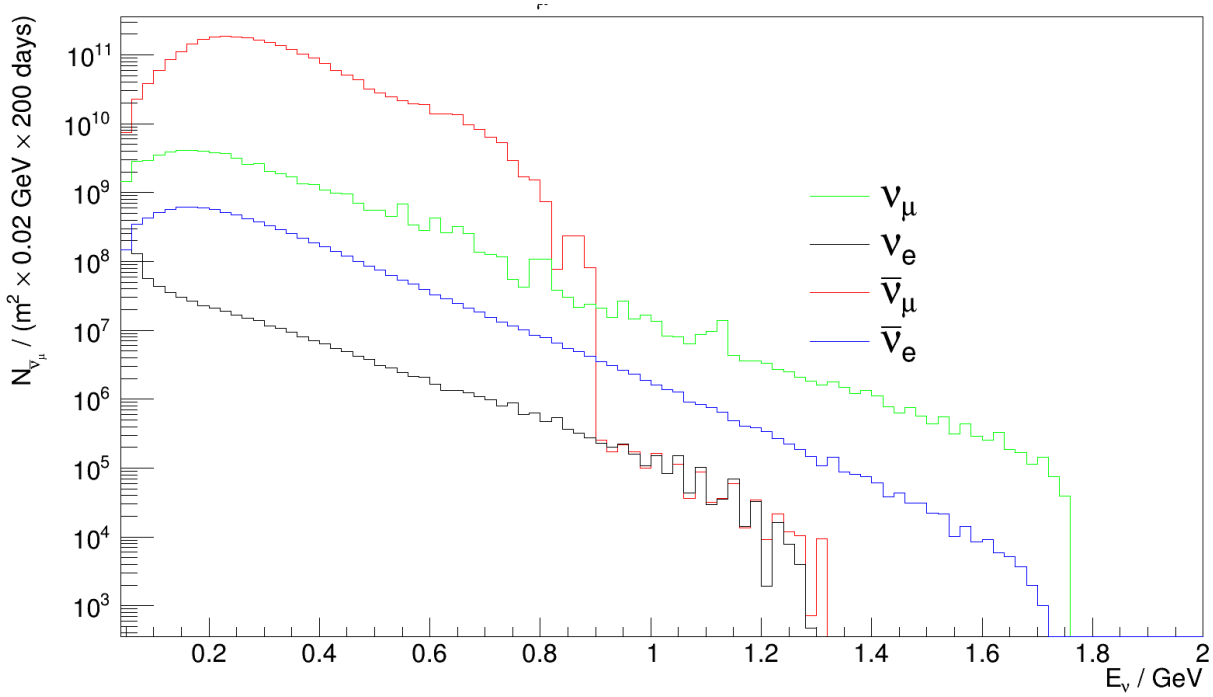

(a)

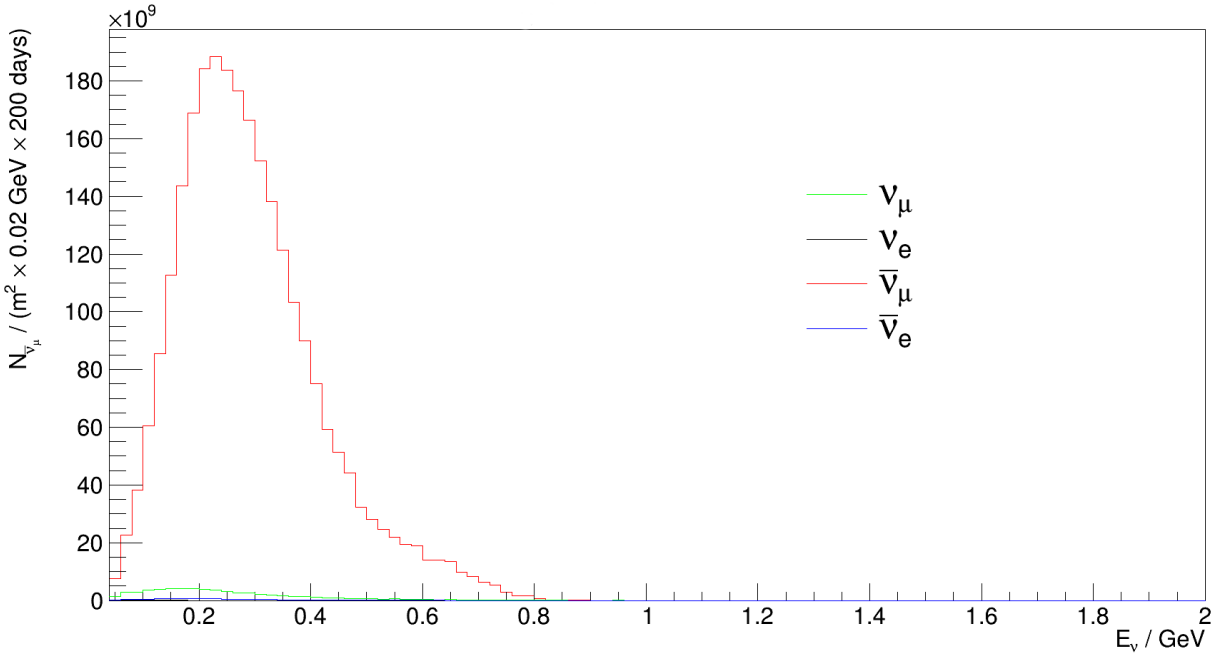

(b)

Figure 4.2: Neutrino fluxes as functions of energy produced in negative polarity mode at 100 km from the source in 200 days

every known interaction, some of which are mentioned in Section 2.5. To get a cross section of the entire molecule, it is enough to add oxygen cross section to two hydrogen

cross sections. The cross section of the entire H_2O molecule can be seen in Fig. 4.3.

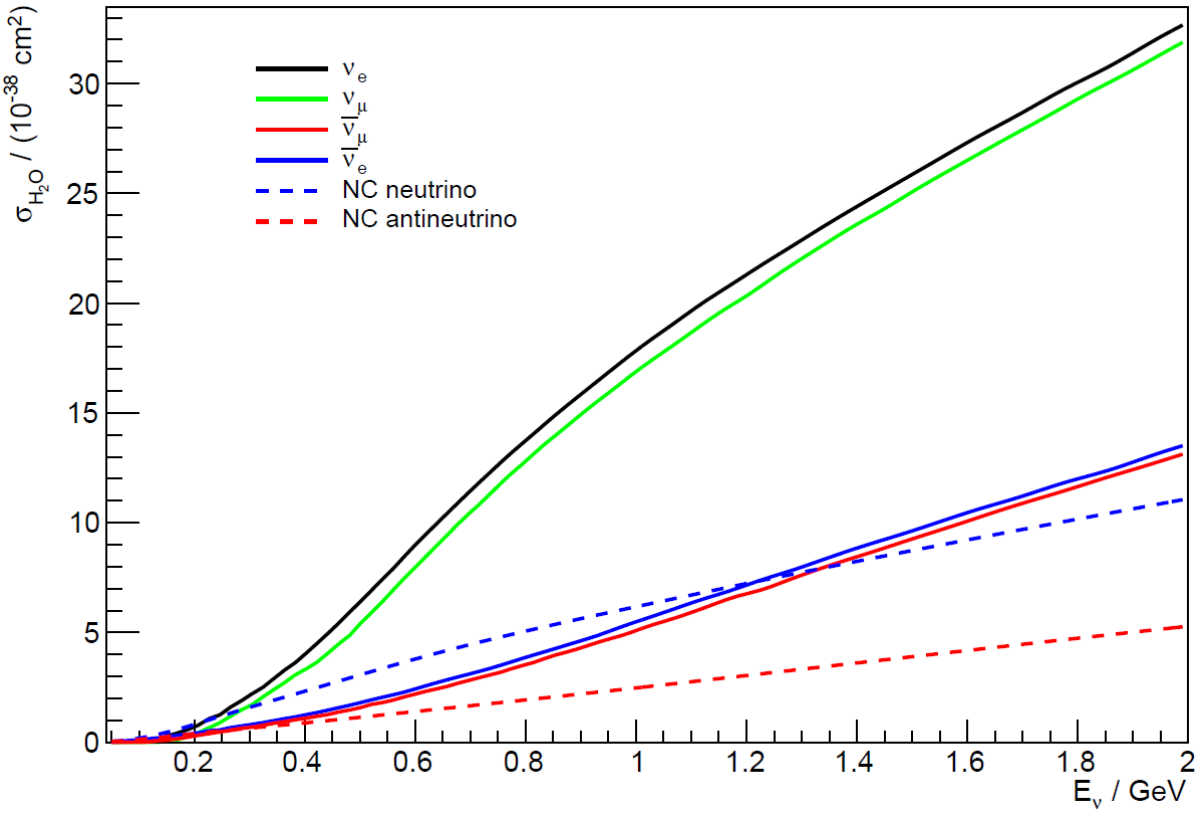

Figure 4.3: Cross section of H_2O molecule as a function of energy procured from GENIE

Notice that cross section of antineutrinos is 2 to 3 times smaller than that of neutrinos. This comes from different processes by which they interact. Namely

$$\nu_\mu + d \longrightarrow \mu^- + u \tag{4.7}$$

and

$$\bar{\nu}_\mu + u \longrightarrow \mu^+ + d\,. \tag{4.8}$$

ratio of these two cross sections (for free massless quarks) results in a factor of 3. In reality, as seen in Fig. 4.3, it is not exactly three. Difference comes from the inclusion of the nucleon model as a whole and quarks and antiquarks coming from the "sea" inside the nucleon.

As the target is not one molecule of water but an entire detector (tank of water), it is desirable to work with a quantity which represents the entire target. This quantity, named as *cross section of a tank of water* is just a multiplication of a cross section of

a single water molecule by the number of water molecules in a tank of water (detector). Number of molecules of water, N, in a tank of mass m can be found as following

$$N = \frac{m}{M(\mathrm{H_2O})} N_A \ , \tag{4.9}$$

where $N_A = 6.022 \times 10^{23}$ is the Avogadro's constant and M is the molar mass calculated as

$$M = 2A_r(\mathrm{H}) + A_r(\mathrm{O}) \ , \tag{4.10}$$

where $A_r(\mathrm{H}) = 1\,\mathrm{g/mol}$ and $A_r(\mathrm{O}) = 16\,\mathrm{g/mol}$. This way, the cross section for any target mass at a specific energy is value given by GENIE as shown in Fig. 4.3 multiplied by N as defined in (4.9).

4.3 Oscillation probability

Flux of a specific flavour of a neutrino is not only dependent on a distance but also on neutrino oscillations. As there exists a probability (as described in sections 2.2 and 2.3) that, for example, starting muon neutrino oscillates to an electron neutrino at the detector. This effect is only applicable for the FarWatCh detector as the NearWatCh detector is too close to the source of neutrinos. Taking this effect into the account is as straight forward as multiplying the starting flux with probability of oscillation for a wanted channel of oscillations.

For clarity, here is an example. The goal is to observe the $\nu_\mu \longrightarrow \nu_e$ oscillation channel. Expected flux of electron neutrinos that originated at the source as a muon neutrino is a multiplication of the original muon neutrino flux with probability of oscillation to electron neutrino.

For these reasons, oscillation probability had to be calculated for each channel. This has been done analytically (in C++) for both vacuum oscillations (Section 2.2) and oscillations in matter[3] (Section 2.3).

[3]For oscillations in matter, analytical solution is possible only for cases where matter density is constant. In the case of ESSνSB, the distance is short enough for neutrino trajectory to go through only one type of rock making density approximately constant.

Parameters used for all calculations are taken from *Particle Data Group* [16].

$$\begin{aligned} \Delta m^2_{31} &= 2.5283 \times 10^{-3}\ \text{eV}^2 \\ \Delta m^2_{32} &= 2.453 \times 10^{-3}\ \text{eV}^2 \\ \Delta m^2_{21} &= 7.53 \times 10^{-5}\ \text{eV}^2 \\ \sin\theta_{31} &= 0.147648213 \\ \sin\theta_{32} &= 0.7382410613 \\ \sin\theta_{21} &= 0.5540755001 \end{aligned} \tag{4.11}$$

The effect of matter effects on neutrino oscillations can be seen in Fig. 4.4. In the figure, probability of oscillation for $\nu_\mu \longrightarrow \nu_e$ is shown. It is clear from the plot that at the first oscillation maximum (located at around 1 GeV) there is a big difference between vacuum probability (full line) and probability with included matter effects (dashed line). Furthermore, the differences in oscillation between different δ_{CP} is not that big, making the measurements less precise. On the other hand, second oscillation maximum (located at around 0.4 GeV) does not depend heavily on matter effects while having bigger sensitivity to different δ_{CP}. It is evident from this that second oscillation maximum is a much better choice for measuring CP violation. One down side is the distance of second oscillation maximum (540 km for 0.4 GeV neutrinos) which results in much smaller flux of neutrinos at the detector. This is one of the reasons all the previous experiments [21] have measured in the first oscillation maximum.

4.3.1 Conversion from electron density to matter density

One technical detail is the matter factor D as introduced in (2.34). It is proportional to concentration of electrons in matter, which can be difficult to determine. For this reason, it is easier to rewrite $D = 2\sqrt{2} \times G_F \times n_e \times E$ to depend on the density of matter.

Starting from a definition of concentration,

$$\begin{aligned} n_e &= \frac{N_e}{V} = \frac{Z \times N_m}{V} \\ &= \frac{Z \times n_m \times N_A}{V} = \frac{Z \times \frac{m}{M_m} \times N_A}{V} = \rho \times \frac{Z}{M_m} \times N_A\ , \end{aligned} \tag{4.12}$$

where N_e is number of electrons, V is volume of matter, Z is a proton number, N_m is a number of molecules in volume V, n_m is number of moles of molecule m in volume V, N_A

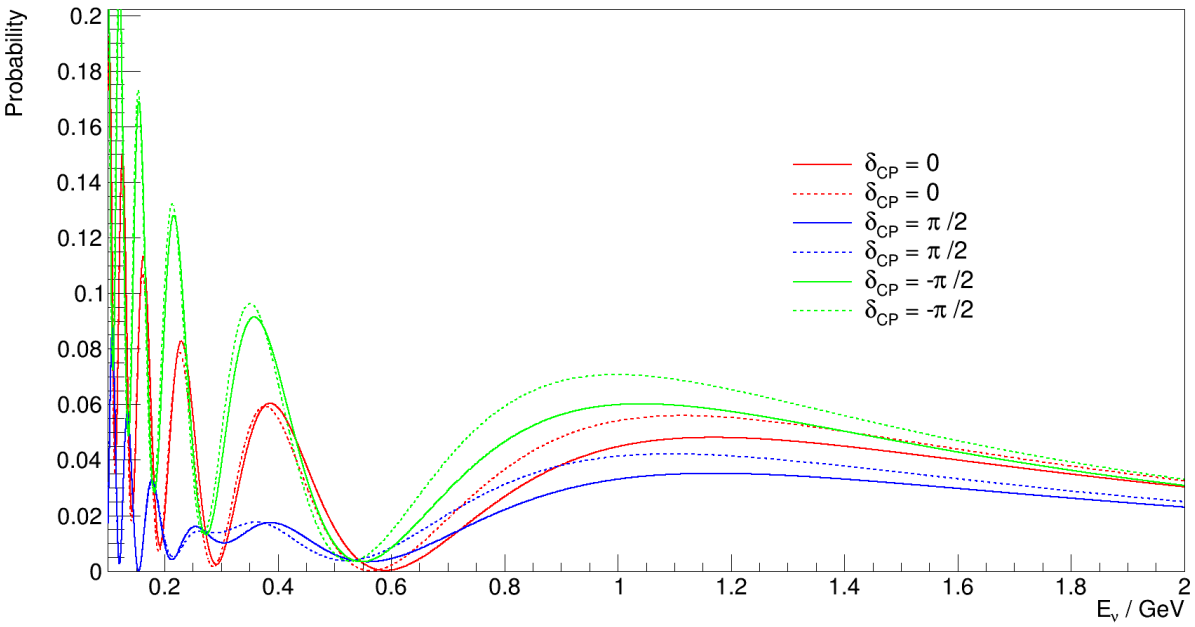

Figure 4.4: Oscillation of probability for $\nu_\mu \longrightarrow \nu_e$ channel as a function of energy. Full lines represent vacuum oscillation probability. Dashed lines represent oscillation probability with included matter effects. Distance is 540 km.

is Avogadro constant, M_m is molar mass of molecule m and ρ is density of matter inside the volume V.

As the Earth's crust is primarily made out of silicon and oxygen [22], a very good approximation is to take that number of protons Z is half of all the nucleons in volume V (as the number of protons and neutrons for most common isotopes of silicon and oxygen are the same), that is

$$\frac{Z}{M_m} \approx \frac{1}{2}; \qquad \left[\frac{1}{\mathrm{g/mol}}\right] = \left[\frac{\mathrm{mol}}{\mathrm{g}}\right] . \tag{4.13}$$

With this, the formula (4.12) takes following form

$$n_e = \frac{\rho N_A}{2} \times \left(\frac{\mathrm{mol}}{\mathrm{g}}\right) , \tag{4.14}$$

and with the $N_A = 6.022 \times 10^{23}$ mol^{-1}, the unit for n_e is $[n_e] = \left[\frac{1}{cm^3}\right]$.

The quantity D is now

$$D = 2\sqrt{2} \times G_F \times \frac{\rho N_A}{2} \times E \times \left(\frac{\mathrm{mol}}{\mathrm{g}}\right) . \tag{4.15}$$

Desired unit for quantity D is $[D] = \left[\mathrm{eV}^2\right]$. With $G_F = 1.16639 \times 10^{-5}$ GeV^{-2} and E given in GeV we will first convert n_e to be in GeV^3. It follows from natural unit conversion

that

$$\hbar c = 1 = 197.327 \text{ MeV fm} . \tag{4.16}$$

From this it is possible to see that conversion from cm to GeV is

$$\text{cm} = \frac{1}{1.97 \times 10^{-14} \text{ GeV}} . \tag{4.17}$$

Inserting this into n_e and D one gets

$$D = 2\sqrt{2} \times G_F \times \frac{\rho N_A}{2} \times (1.97 \times 10^{-14})^3 \times E \times \left(\frac{\text{mol} \times \text{GeV}^3 \times \text{cm}^3}{\text{g}} \right) . \tag{4.18}$$

Multiplying all the constants and converting to eV^2 with $\text{GeV}^2 = 10^{18}\text{eV}^2$ gives the final formula for matter factor D depending on matter density as

$$D = 7.5945 \times 10^{-5} \times \rho \times E \times \left(\frac{\text{cm}^3 \times \text{eV}^2}{\text{g} \times \text{GeV}} \right) . \tag{4.19}$$

The value used for all calculations (in accordance with [23]) is,

$$\rho = 2.8 \, \text{g/cm}^3 . \tag{4.20}$$

4.4 Near Detectors

4.4.1 Near Water Cherenkov Detector

NearWatCh detector is placed 250 m from the source of the neutrino production target. This means neutrino oscillations play no role in neutrino flux. For this reason no modifications to the original flux are needed other than scaling due to distance. Mass of the detector is 500 t. Number of expected neutrino interactions in time T at the NearWatCh is then calculated as

$$N = N_\text{t} \times T \times \int_{E_1}^{E_2} F(E) \times \sigma(E) \text{d}E . \tag{4.21}$$

Evaluating this integral is not trivial in C++ and ROOT because flux F and cross section σ are two different ROOT functions. Flux data is structured in histogram format (TH1D ROOT function) while the cross section is in the format of a continuous function (TGraph ROOT function). Multiplying these two ROOT functions point-by-point gives as a result

a continuous function with multiple singularities which then is a problem for the built in *Integral()* function in C++ as it does not handle singularities well. The singularities originate from sudden changes of values at the edges of bins of a flux histogram. Example of this resulting function can be seen in Fig. 4.5. With the integral function being defined as

$$g(x) = \int_0^x f(x')\mathrm{d}x' \,, \tag{4.22}$$

where $f(x)$ is the function obtained by multiplying the flux and cross-section. Solution for this integration problem is to write an algorithm for so called *bin-to-bin* integration method. In this method, integration is preformed in separate intervals which correspond to the bins in the flux histogram. This way one can avoid sudden changes at the edges of the bins. Furthermore, as the result of each integrated bin is only one number, it can be placed inside of a new histogram in its own bin which then at the end gives us a histogram where in each bin is the number of expected interactions for that energy range (bin range). Summation of all bins gives us a total expected number of interactions.

The subintegral function in (4.9) will be referred to as

$$\frac{\mathrm{d}R}{\mathrm{d}E} \equiv F(E) \times \sigma(E) \,, \tag{4.23}$$

where this quantity will be further scaled depending on the number of targets N_t and time observed T. This quantity has been plotted for all channels using the flux provided by the project and cross section taken from GENIE (Fig. 4.6 and Fig. 4.7). The exact numbers calculated are shown in Table 1 and Table 2 for positive and negative polarity respectively.

As can be seen in Tables 1 and 2, quantity *Pile up chance* has also been calculated for a $\frac{1}{4}$ pulse. As mentioned in Section 3, neutrino beam will produce pulses of neutrinos which will be directed at the detectors. Each of these pulses will be additionally "chopped" into 4 smaller pulses. A possible problem here is if two neutrinos from this quarter pulse interact at the same detector. It would then be impossible to differentiate two events, and those events would have to be ignored which means losing statistics. Fortunately, pile up chance is very small and should not lower the statistics significantly. Over 27 million events are expected for muon neutrinos in 200 days of positive horn polarity, which is a big

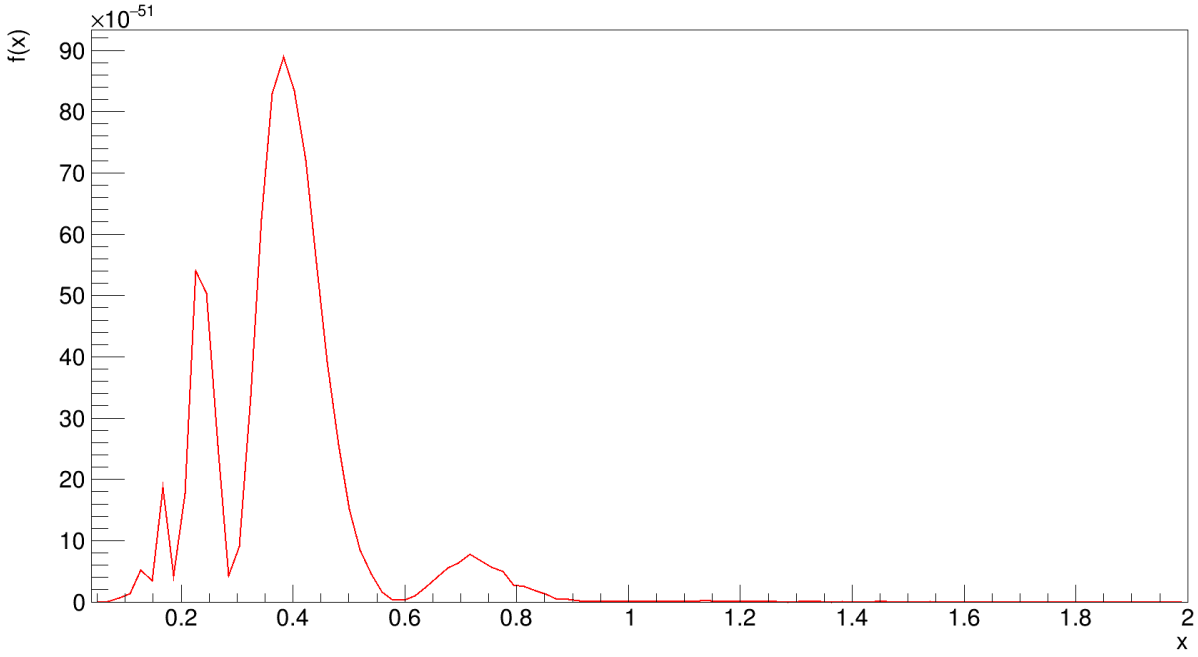

(a)

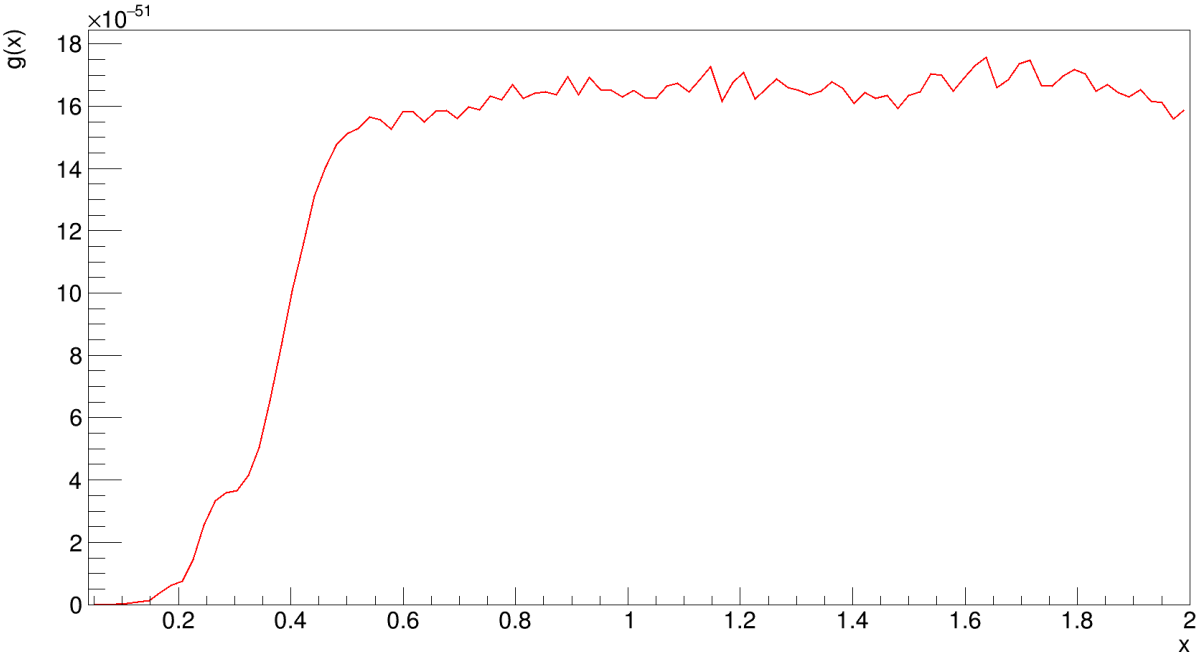

(b)

Figure 4.5: Illustration of the problem of integrating non-smooth function. Top panel (a) is the resulting function of multiplying ROOT TH1D histogram and continuous TGraph function. Bottom panel (b) is the integral function of this function. The bottom plot should be monotonically rising if the integration is preformed correctly.

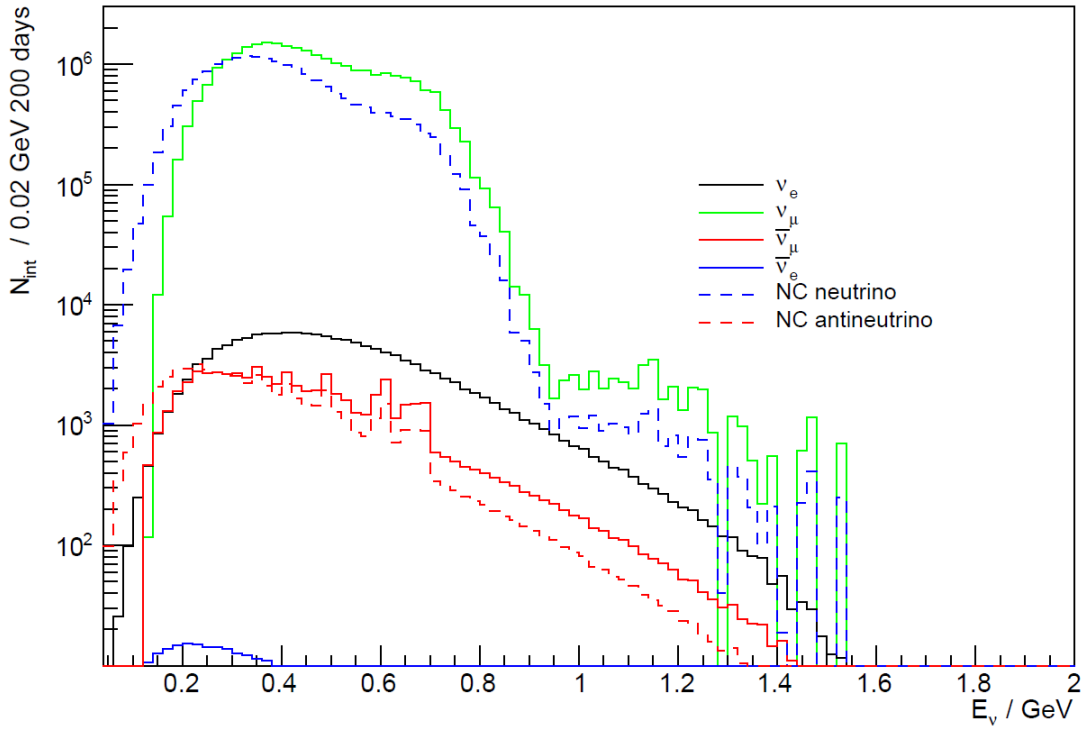

Figure 4.6: Number of neutrino interactions as a function of energy at NearWatCh (250 m) for 200 days observation and positive horn polarity.

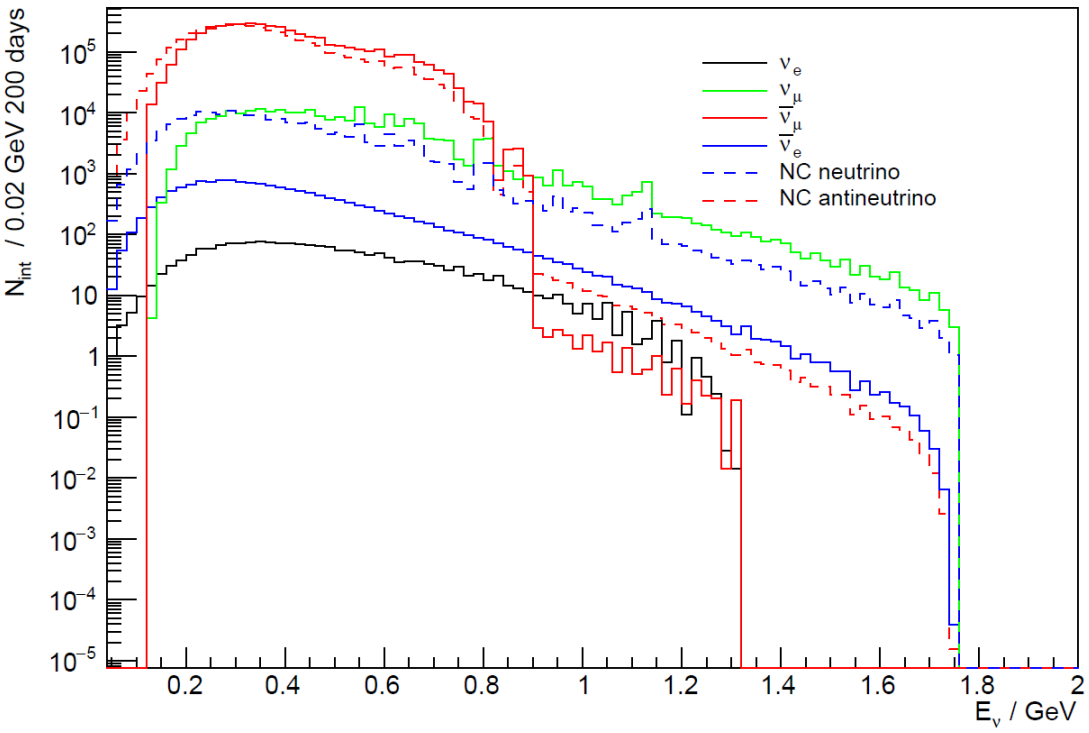

Figure 4.7: Number of neutrino interactions as a function of energy at NearWatCh (250 m) for 200 days observation and negative horn polarity.

	Time	Distance	ν_μ	ν_e	$\overline{\nu}_\mu$	$\overline{\nu}_e$
CC	200 days	250 m	27 366 600	148 172	64 471	303
		500 m	6 841 650	37 043	16 118	76
	Pile up chance (1/4 pulse)	250 m	$3.9 \times 10^{-2}\%$	$1.2 \times 10^{-6}\%$	$2.2 \times 10^{-7}\%$	~ 0 %
		500 m	$2.5 \times 10^{-3}\%$	$7.4 \times 10^{-8}\%$	$1.4 \times 10^{-8}\%$	~ 0 %
NC	200 days	250 m	19 914 500	84 584	58 827	240
		500 m	4 978 625	21 146	14 707	60
	Pile up chance (1/4 pulse)	500 m	$2.1 \times 10^{-2}\%$	$3.8 \times 10^{-7}\%$	$1.8 \times 10^{-7}\%$	~ 0 %
		250 m	$1.3 \times 10^{-3}\%$	$2.4 \times 10^{-8}\%$	$1.2 \times 10^{-8}\%$	~ 0 %

Table 1: Expected number of neutrino interactions at the NearWatCh detector for positive horn polarity given the flux and cross section shown in Fig. 4.1 and Fig. 4.3 respectively.

	Time	Distance	ν_μ	ν_e	$\overline{\nu}_\mu$	$\overline{\nu}_e$
CC	200 days	250 m	250 172	1 852	4 761 560	15 336
		500 m	62 543	463	1 190 390	3 834
	Pile up chance (1/4 pulse)	250 m	$3.3 \times 10^{-6}\%$	~ 0 %	$1.2 \times 10^{-3}\%$	$1.3 \times 10^{-8}\%$
		500 m	$2.4 \times 10^{-7}\%$	~ 0 %	$7.4 \times 10^{-5}\%$	~ 0 %
NC	200 days	250 m	198 113	1 236	4 273 830	11 533
		500 m	49 528	309	1 068 458	2 883
	Pile up chance (1/4 pulse)	500 m	$2.1 \times 10^{-6}\%$	~ 0 %	$9.7 \times 10^{-4}\%$	$7.1 \times 10^{-9}\%$
		250 m	$1.4 \times 10^{-7}\%$	~ 0 %	$6.1 \times 10^{-5}\%$	~ 0 %

Table 2: Expected number of neutrino interactions at the NearWatCh detector for negative horn polarity given the flux and cross section shown in Fig. 4.2 and Fig. 4.3 respectively.

sample size. This will be used to determine the cross-sections more precisely, as for these low energies cross section have big uncertainties. It will also provide a much more precise information about the flux that will be used for calculations at the FarWatCh. In combination, better knowledge of the cross section and flux will lower systematic uncertainties of the experiment.

4.4.2 Super Fine-Grained Detector

Super Fine-Grained Detector (SFGD) will be used along side the NearWatCh to improve energy and path reconstruction of neutrinos. The SFGD will be made out of a large number of small scintillator cubes. Chemical composition of these cubes will be C_8H_8 and $C_{18}H_{14}$ (similar to [24]) where C_8H_8 is the dominant scintillator. Total mass of the SFGD is 1030 kg with a mass ratio of $m_{C_8H_8} : m_{C_{18}H_{14}} = 0.985 : 0.015$ which corresponds to

$$m_{C_8H_8} = 1014.55\,\text{kg} \quad ; \quad m_{C_{18}H_{14}} = 15.45\,\text{kg}\,. \tag{4.24}$$

Calculation of expected number of interactions is performed in the similar way as in the case of NearWatCh with the only difference being the cross section used. The calculation was split into two part, first calculating the expected interactions on all of the C_8H_8 molecules and then calculating the expected interactions on all of the $C_{18}H_{14}$ where the total number of interactions is the sum of these two. The cross section for individual molecules can be seen in Fig. 4.8 while the exact numbers of expected neutrino oscillations can be seen in Table 3 and Table 4 for positive and negative horn polarity, respectively.

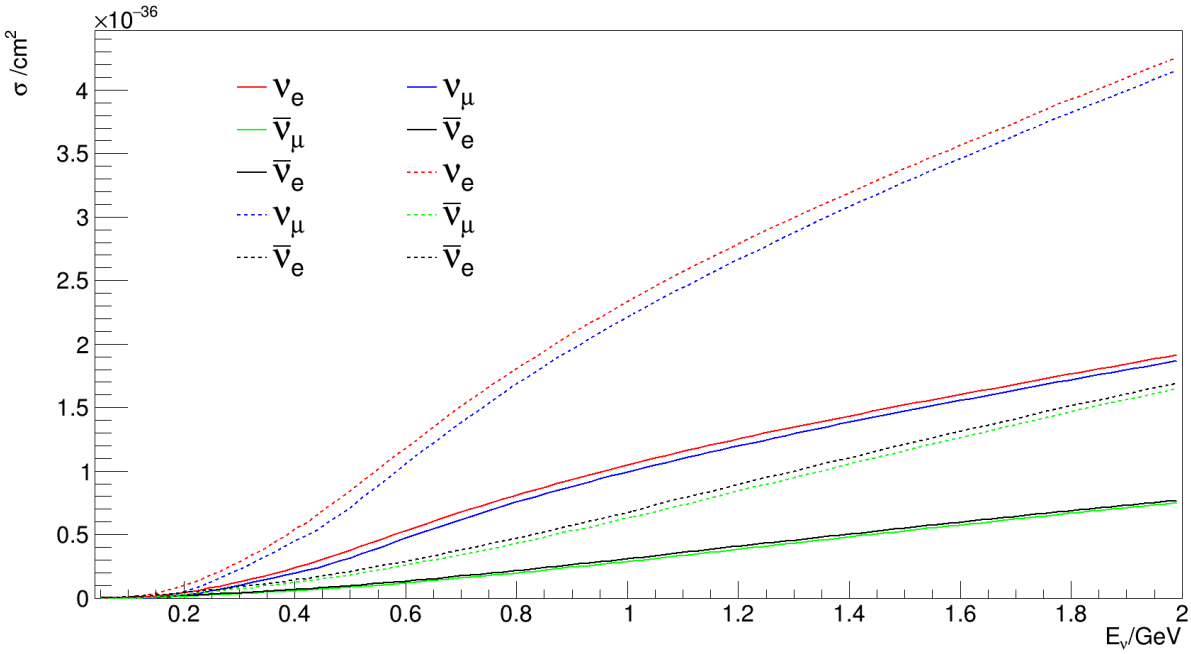

Figure 4.8: Cross section of neutrino CC interactions with C_8H_8 molecule (full line) and $C_{18}H_{14}$ molecule (dashed line) as a function of energy.

	Time	Molecule	ν_μ	ν_e	$\bar{\nu}_\mu$	$\bar{\nu}_e$
CC	200 days	C_8H_8	57 334.5	309.2	120.7	0.6
		$C_{18}H_{14}$	828.7	4.5	1.6	0.01
		Total	58 163.3	313.6	122.3	0.6
NC	200 days	C_8H_8	39 471	167.7	117.0	0.5
		$C_{18}H_{14}$	560.9	2.4	1.8	0.01
		Total	40 031.9	170.1	118.8	0.5

Table 3: Expected number of events for positive horn polarity at SFGD. Operating at positive horn polarity at a distance of 250 m from the neutrino production target

	Time	Molecule	ν_μ	ν_e	$\bar{\nu}_\mu$	$\bar{\nu}_e$
CC	200 days	C_8H_8	524.3	3.9	8 888.4	28.7
		$C_{18}H_{14}$	7.6	0.1	120.9	0.4
		Total	531.9	3.9	9.009.3	29.1
NC	200 days	C_8H_8	391.2	2.4	8 336.2	22.4
		$C_{18}H_{14}$	5.6	0.03	117.9	0.3
		Total	396.7	2.5	8 454.1	22.8

Table 4: Expected number of events for negative horn polarity at SFGD. Operating at negative horn polarity at a distance of 250 m from the neutrino production target

4.5 Far Water Cherenkov Detector

Unlike near detectors, FarWatCh is placed further away from the neutrino source (either 540 km or 360 km) and this means that neutrino oscillations must be considered. Hence, modification of the flux of neutrinos is required. This is done by multiplying the flux at the distance of the detector with probability for neutrino oscillation channel we are interested in (as described in Section 4.3). Example of this can be seen oin Fig. 4.9 for the $\nu_\mu \rightarrow \nu_e$ channel. Oscillated fluxes at a distance of 540 km and for $\delta_{CP} = 0$ are shown in Fig. 4.10 and Fig. 4.11 for positive and negative polarity, respectively.

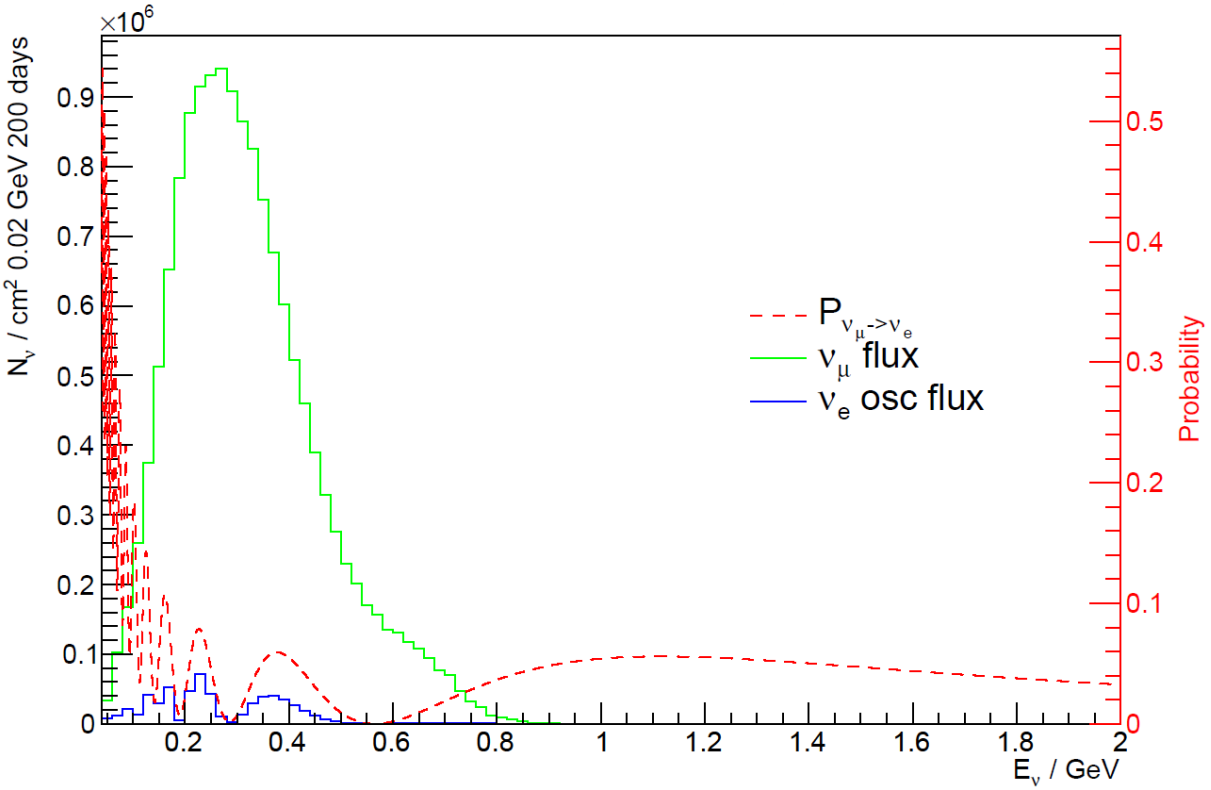

Figure 4.9: Green line indicates the original flux of muon neutrinos as a function of energy scaled to the distance of FarWatCh. Dotted red line is the probability of oscillation as a function of energy for $\nu_\mu \to \nu_e$ channel. Blue line is the final oscillated flux of electron neutrinos as a function of energy with which further calculations are made. Matter effects are included and $\delta_{CP} = 0$ is assumed.

Because of the additional factor of probability, equation (4.3) takes the form

$$N = N_{\mathrm{t}} \times T \times \int_{E_1}^{E_2} F(E) \times P(E) \times \sigma(E) \mathrm{d}E \ ,$$

where $F(E)$ is the original flux and $P(E)$ is the probability of oscillation. Here one needs to be careful which cross section to use. In the case of NearWatCh, a neutrino which was created at the source was the same neutrino (same flavour) which interacted in the detector. Here this is not necessarily the case. No matter which neutrino is the original from the source, cross section used is purely dictated by the neutrino which interacted at the detector, i.e. the neutrino into which the original neutrino oscillated.

In analogy with Section 4.4.1, one can introduce the quantity

$$\frac{\mathrm{d}R}{\mathrm{d}E} \equiv F(E) \times P(E) \times \sigma(E) \ , \tag{4.25}$$

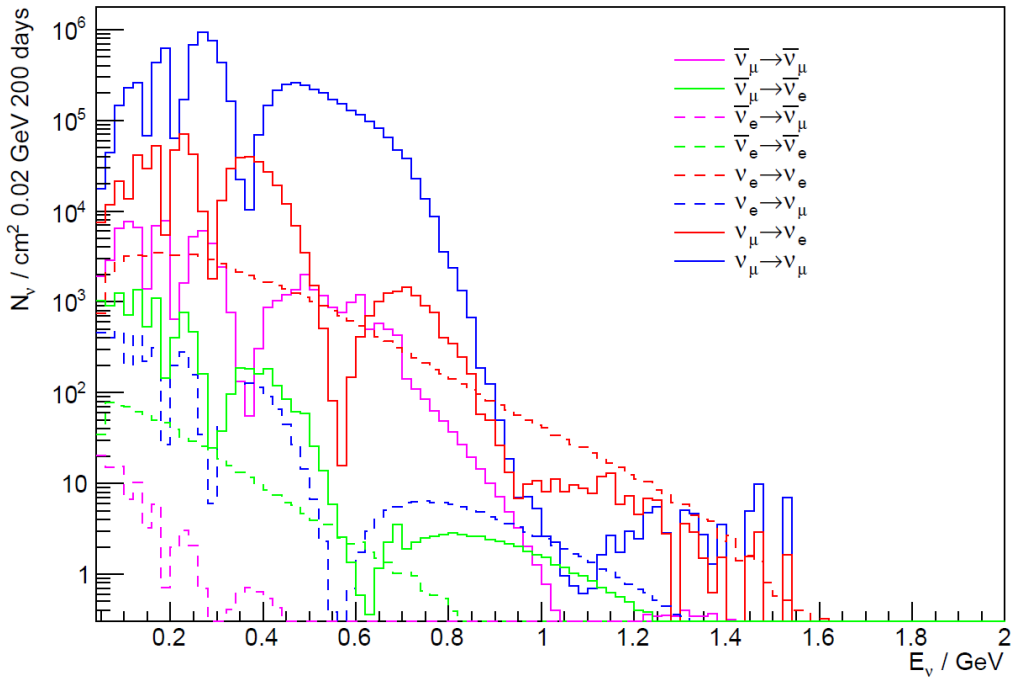

Figure 4.10: Oscillated flux as a function of energy for all channels at a distance of 540 km and $\delta_{CP} = 0$ for positive polarity. Matter effects are included and $\delta_{CP} = 0$ is assumed.

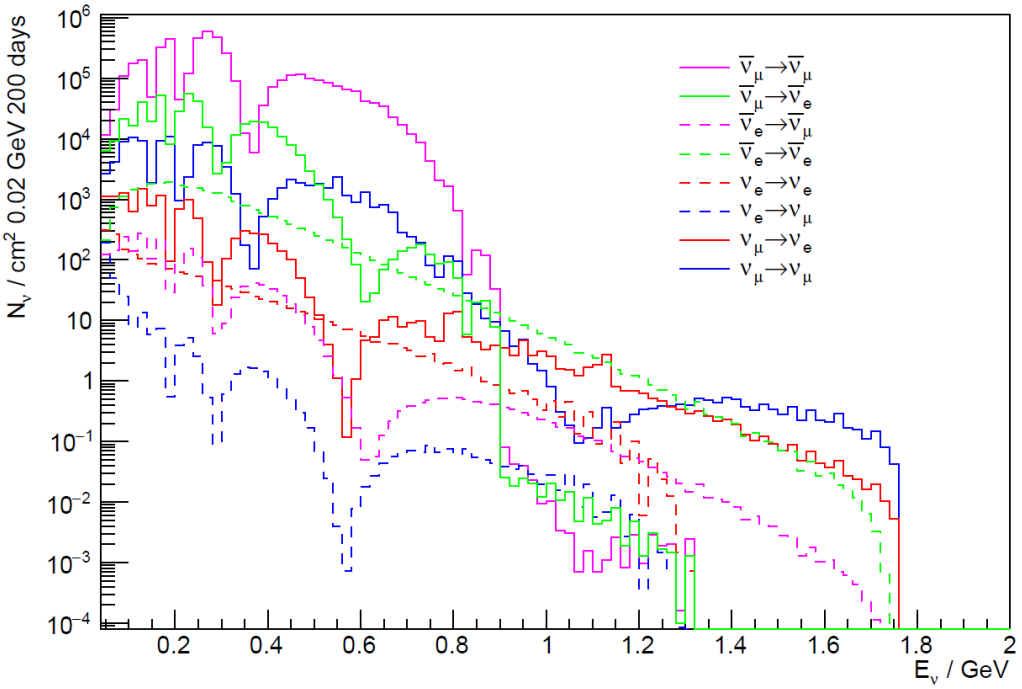

Figure 4.11: Oscillated flux as a function of energy for all channels at a distance of 540 km and $\delta_{CP} = 0$ for negative polarity. Matter effects are included and $\delta_{CP} = 0$ is assumed.

where now the oscillation probability is taken into the account. Again, example of $\nu_\mu \to \nu_e$ channel is shown in Fig. 4.12, while $\frac{dR}{dE}$ for all channels is shown in Fig. 4.13 and Fig. 4.14 for positive and negative polarity respectively.

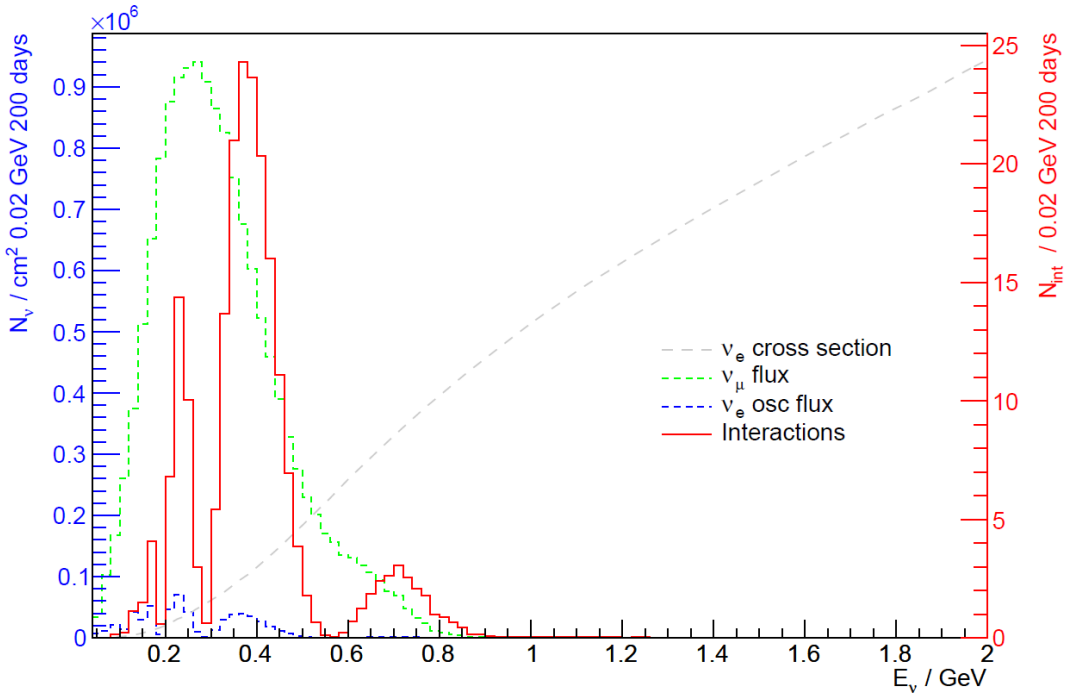

Figure 4.12: Green dotted line represents the original flux of muon neutrinos as a function of energy. Blue dotted line is oscillated flux of electron neutrinos as a function of energy. Grey dotted line is the cross section of electron neutrino and a water molecule as a function of energy and red line is number of interactions as a function of energy. Matter effects are included and $\delta_{CP} = 0$ is assumed.

From the Table 5 it is possible to see that the highest number of interactions for positive horn polarity are the NC interactions of neutrinos, closely followed by the CC interactions of neutrinos coming from the $\nu_\mu \to \nu_\mu$ channel. $\nu_\mu \to \nu_e$ channel is the signal and has the third most interactions.

Similar conclusions can be made from Fig. 4.14 where one can see that NC interactions of antineutrinos are the highest closely followed by the CC interactions of the antineutrinos coming from the $\bar{\nu}_\mu \to \bar{\nu}_\mu$ channel. Here the signal are the antineutrinos coming from the $\bar{\nu}_\mu \to \bar{\nu}_e$ channel and as expected they are the third highest interactions. It would be impossible to get the signal interactions to be more numerous than those from the

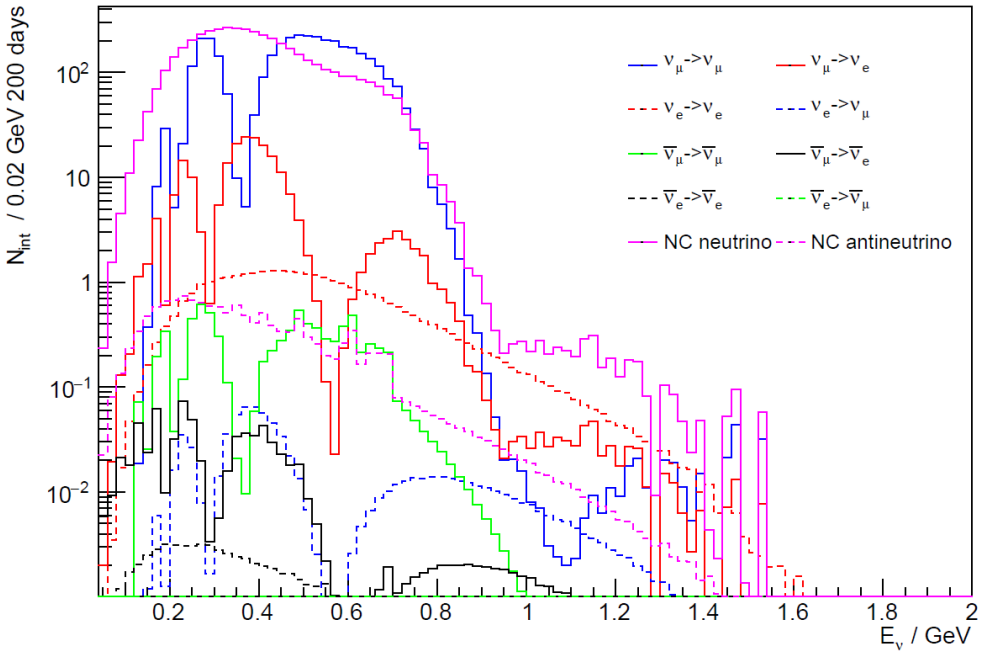

Figure 4.13: Expected number of interaction as a function of energy for all channels at FarWatCh in 200 day of observation for positive polarity. Matter effects are included and $\delta_{CP} = 0$ is assumed.

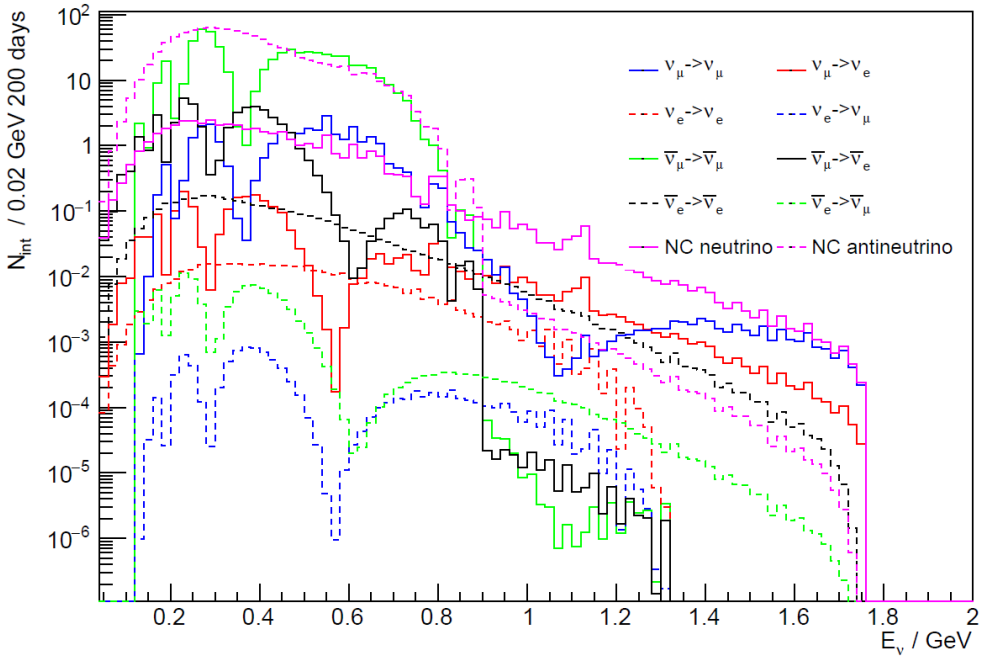

Figure 4.14: Expected number of interaction as a function of energy for all channels at FarWatCh in 200 days of observation for negative polarity. Matter effects are included and $\delta_{CP} = 0$ is assumed.

$\bar{\nu}_\mu \to \bar{\nu}_\mu$ channel as the oscillation probability for appearance channel is a lot smaller then the disappearance channel.

	Channel	Non Oscillated	Oscillated		
			$\delta_{CP} = 0$	$\delta_{CP} = \pi/2$	$\delta_{CP} = -\pi/2$
CC	$\nu_\mu \to \nu_\mu$	6 311.4	3 593.6 (3 580.7)	3 581.8 (3 584.1)	3 581.8 (3 584.1)
	$\nu_\mu \to \nu_e$	0	213.7 (221.2)	98.1 (88.3)	350.8 (334.7)
	$\nu_e \to \nu_e$	34.2	32.1 (32.3)	32.1 (32.3)	32.1 (32.3)
	$\nu_e \to \nu_\mu$	0	0.8 (0.8)	1.3 (1.2)	0.4 (0.4)
	$\overline{\nu}_\mu \to \overline{\nu}_\mu$	14.9	7.9 (7.9)	7.9 (7.9)	7.9 (7.9)
	$\overline{\nu}_\mu \to \overline{\nu}_e$	0	0.7 (0.7)	1.0 (1.0)	0.3 (0.3)
	$\overline{\nu}_e \to \overline{\nu}_e$	0.07	0.06 (0.06)	0.06 (0.06)	0.06 (0.06)
	$\overline{\nu}_e \to \overline{\nu}_\mu$	0	0.002 (0.002)	0.0006 (0.0007)	0.003 (0.003)
NC	ν_μ	4 592.8			
	ν_e	19.5			
	$\overline{\nu}_\mu$	13.6			
	$\overline{\nu}_e$	13.6			

Table 5: Expected number of interactions at FarWatCh for all channels in 200 days of observation time during positive horn polarity with (without) included matter effects.

The exact numbers for positive horn polarity are shown in Table 5. The "Non Oscillated" column gives a number of interactions in case if there were no neutrino oscillations. The next three columns give the number of neutrinos that would interact for a given δ_{CP}. The value of $\frac{\pi}{2}$ and $-\frac{\pi}{2}$ are chosen because they indicate the maximal violation of CP symmetry and will give the highest variation of neutrino interaction compared to the case when the CP symmetry is conserved ($\delta_{CP} = 0$). From these numbers few different things can be concluded. First it confirms the previous statement that disappearance channels are not sensitive to CP symmetry violation and the δ_{CP} can not be measured using disappearance channels. Another thing is that there is a clear difference in the expected interactions for different δ_{CP} in the signal channel. This is a good thing as this difference can be used to measure the CP symmetry with more precision. For example if the expected number of interactions for all values of δ_{CP} is the same or similar, it would be

	Channel	Non Oscillated	Oscillated		
			$\delta_{CP} = 0$	$\delta_{CP} = \pi/2$	$\delta_{CP} = -\pi/2$
CC	$\nu_\mu \to \nu_\mu$	57.7	32.1 (31.9)	32.0 (31.9)	32.0 (31.9)
	$\nu_\mu \to \nu_e$	0	2.1 (2.2)	1.0 (0.9)	3.5 (3.3)
	$\nu_e \to \nu_e$	0.43	0.4 (0.4)	0.4 (0.4)	0.4 (0.4)
	$\nu_e \to \nu_\mu$	0	0.009 (0.009)	0.02 (0.01)	0.005 (0.004)
	$\overline{\nu}_\mu \to \overline{\nu}_\mu$	1 098.1	579.2 (582.5)	582.6 (583.3)	582.6 (583.3)
	$\overline{\nu}_\mu \to \overline{\nu}_e$	0	47.0 (45.0)	66.3 (69.4)	16.2 (16.6)
	$\overline{\nu}_e \to \overline{\nu}_e$	3.5	3.3 (3.3)	3.3 (3.3)	3.3 (3.3)
	$\overline{\nu}_e \to \overline{\nu}_\mu$	0	0.09 (0.09)	0.04 (0.04)	0.1 (0.1)
NC	ν_μ	45.7			
	ν_e	0.3			
	$\overline{\nu}_\mu$	985.6			
	$\overline{\nu}_e$	2.7			

Table 6: Expected number of interactions at FarWatCh for all channels in 200 days of observation time during negative horn polarity with (without) included matter effects.

hard to say if the slight deviation from the expected number of interaction in the $\delta_{CP} = 0$ case is because of CP asymmetry or a random chance. The higher the relative difference, the easier it is to measure the CP violation with higher significance. This is one of the main reasons why the ESSνSB project is designed to measure at the second oscillation maximum.

Similar thing can be said for the expected negative horn polarity measurements whose numbers are shown in Table 6. As the overall numbers are smaller, the difference is also smaller, but the relative difference remains similar. This is also a good sign for the measurement possibility.

Comparing the case where matter effects were included for calculations and the case where the matter effects were not included, one can see what was already expected. The difference in expected interactions is modest, which means that matter effects do not have

a significant effect in the second oscillation maximum as was hinted at with Fig. 4.4. This makes the approximation of the Earth's matter density less important as any uncertainty from this approximation would not have an enormous impact into the expected number of interaction.

5 Conclusion

The ESSνSB project aims to observe CP violation in the $\nu_\mu \rightarrow \nu_e$ ($\overline{\nu}_\mu \rightarrow \overline{\nu}_e$) appearance channel. Before the project itself starts to collect data, it needs to simulate the data to predict the possible performance of the project. One of the key components in these simulations is to know the expected number of neutrino interactions in the detectors. This thesis presented expected number of interactions that will be used to simulate further data for evaluating possible performance of ESSνSB project. For the numbers alone, results (Table 5 and Table 6) show that 2nd oscillation maximum in combination with given flux produces a noticeable difference in expected number of interactions for different δ_{CP}. In addition, results also show that 2nd oscillation maximum is not overly dependant on matter effects in neutrino oscillations (Fig. 4.4) which is an advantage as the exact matter density is often difficult to determine and is often not homogeneous.

References

[1] A. Alekou et al. "Updated physics performance of the ESSnuSB experiment". In: (June 2021). arXiv: 2107.07585 [hep-ex].

[2] Carlo Giunti and Chung W. Kim. *Fundamentals of Neutrino Physics and Astrophysics*. 2007. ISBN: 978-0-19-850871-7.

[3] Ziro Maki, Masami Nakagawa, and Shoichi Sakata. "Remarks on the Unified Model of Elementary Particles". In: *Progress of Theoretical Physics* 28.5 (Nov. 1962), pp. 870–880. ISSN: 0033-068X. DOI: 10.1143/PTP.28.870. eprint: https://academic.oup.com/ptp/article-pdf/28/5/870/5258750/28-5-870.pdf. URL: https://doi.org/10.1143/PTP.28.870.

[4] Raymond Davis Jr., Don S. Harmer, and Kenneth C. Hoffman. "Search for neutrinos from the sun". In: *Phys. Rev. Lett.* 20 (1968), pp. 1205–1209. DOI: 10.1103/PhysRevLett.20.1205.

[5] Y. Fukuda et al. "Evidence for oscillation of atmospheric neutrinos". In: *Phys. Rev. Lett.* 81 (1998), pp. 1562–1567. DOI: 10.1103/PhysRevLett.81.1562. arXiv: hep-ex/9807003.

[6] Q. R. Ahmad et al. "Direct evidence for neutrino flavor transformation from neutral current interactions in the Sudbury Neutrino Observatory". In: *Phys. Rev. Lett.* 89 (2002), p. 011301. DOI: 10.1103/PhysRevLett.89.011301. arXiv: nucl-ex/0204008.

[7] H. W. Zaglauer and K. H. Schwarzer. "The Mixing Angles in Matter for Three Generations of Neutrinos and the Msw Mechanism". In: *Z. Phys. C* 40 (1988), p. 273. DOI: 10.1007/BF01555889.

[8] J. P. Lees et al. "Observation of Time Reversal Violation in the B^0 Meson System". In: *Phys. Rev. Lett.* 109 (2012), p. 211801. DOI: 10.1103/PhysRevLett.109.211801. arXiv: 1207.5832 [hep-ex].

[9] A. Pich. "CP violation". In: *ICTP Ser. Theor. Phys.* 10 (1994). Ed. by E. Gava et al., pp. 14–42. arXiv: hep-ph/9312297.

[10] David Griffiths. *Introduction to elementary particles*. 2008. ISBN: 978-3-527-40601-2.

[11] F. Vannucci. "Interactions of neutrinos with matter". In: *Prog. Part. Nucl. Phys.* 95 (2017), pp. 1–47. DOI: 10.1016/j.ppnp.2017.03.003.

[12] E. Baussan et al. "A very intense neutrino super beam experiment for leptonic CP violation discovery based on the European spallation source linac". In: *Nucl. Phys. B* 885 (2014). Ed. by Norman A. Graf, Michael E. Peskin, and Jonathan L. Rosner, pp. 127–149. DOI: 10.1016/j.nuclphysb.2014.05.016. arXiv: 1309.7022 [hep-ex].

[13] Budimir Klicek. "The ESSnuSB project". In: *PoS* ICHEP2020 (2021), p. 152. DOI: 10.22323/1.390.0152.

[14] Marcos Dracos. "Status of the ESS neutrino Super Beam". In: *PoS* NuFact2017 (2018), p. 017. DOI: 10.22323/1.295.0017.

[15] Joochun Park et al. "Status of the detector design studies for ESSνSB". In: *PoS* NuFact2019 (2020), p. 041. DOI: 10.22323/1.369.0041.

[16] P.A. Zyla et al. "Review of Particle Physics". In: *PTEP* 2020.8 (2020), p. 083C01. DOI: 10.1093/ptep/ptaa104.

[17] R. Brun and F. Rademakers. "ROOT: An object oriented data analysis framework". In: *Nucl. Instrum. Meth. A* 389 (1997). Ed. by M. Werlen and D. Perret-Gallix, pp. 81–86. DOI: 10.1016/S0168-9002(97)00048-X.

[18] C. Andreopoulos et al. "The GENIE Neutrino Monte Carlo Generator". In: *Nucl. Instrum. Meth. A* 614 (2010), pp. 87–104. DOI: 10.1016/j.nima.2009.12.009. arXiv: 0905.2517 [hep-ph].

[19] Costas Andreopoulos et al. "The GENIE Neutrino Monte Carlo Generator: Physics and User Manual". In: (Oct. 2015). arXiv: 1510.05494 [hep-ph].

[20] Júlia Tena-Vidal et al. "Neutrino-Nucleon Cross-Section Model Tuning in GENIE v3". In: (Apr. 2021). arXiv: 2104.09179 [hep-ph].

[21] K. Abe et al. "Search for CP Violation in Neutrino and Antineutrino Oscillations by the T2K Experiment with 2.2×10^{21} Protons on Target". In: *Phys. Rev. Lett.* 121.17 (2018), p. 171802. DOI: 10.1103/PhysRevLett.121.171802. arXiv: 1807.07891 [hep-ex].

[22] John R. Rumble, Thomas J. Bruno, and Maria Doa. *CRC handbook of chemistry and physics: a ready-reference book of chemical and physical data*. CRC Press, 2020.

[23] M. Blennow et al. "Physics potential of the ESSνSB". In: *The European Physical Journal C* 80.3 (2020). ISSN: 1434-6052. DOI: 10.1140/epjc/s10052-020-7761-9. URL: http://dx.doi.org/10.1140/epjc/s10052-020-7761-9.

[24] A. Blondel et al. "A fully-active fine-grained detector with three readout views". In: *Journal of Instrumentation* 13.02 (Feb. 2018), P02006–P02006. ISSN: 1748-0221. DOI: 10.1088/1748-0221/13/02/p02006. URL: http://dx.doi.org/10.1088/1748-0221/13/02/P02006.